Coastal Protection and Restoration Authority
150 Terrace Avenue, Baton Rouge, LA 70802 | coastal@la.gov | www.coastal.la.gov

2017 Coastal Master Plan

Attachment C3-2: Marsh Edge Erosion

Report: Final

Date: April 2017

Prepared By: Mead Allison (The Water Institute of the Gulf), Jim Chen (Louisiana State University), Brady Couvillion (U.S. Geological Survey), Angelina Freeman (Coastal Protection and Restoration Authority), Mark Leadon (Coastal Protection and Restoration Authority), Alex McCorquodale (University of New Orleans), Ehab Meselhe (The Water Institute of the Gulf), Cyndhia Ramatchandirane (The Water Institute of the Gulf), Denise Reed (The Water Institute of the Gulf), and Eric White (The Water Institute of the Gulf).

Coastal Protection and Restoration Authority

This document was prepared in support of the 2017 Coastal Master Plan being prepared by the Coastal Protection and Restoration Authority (CPRA). CPRA was established by the Louisiana Legislature in response to Hurricanes Katrina and Rita through Act 8 of the First Extraordinary Session of 2005. Act 8 of the First Extraordinary Session of 2005 expanded the membership, duties and responsibilities of CPRA and charged the new authority to develop and implement a comprehensive coastal protection plan, consisting of a master plan (revised every five years) and annual plans. CPRA's mandate is to develop, implement, and enforce a comprehensive coastal protection and restoration master plan.

Suggested Citation:

Allison, M., Chen, Q.J., Couvillion, B., Freeman, A., Leadon, M., McCorquodale, A., Meselhe, E., Ramatchandirane, C., Reed, D., and White, E. (2017). *2017 Coastal Master Plan: Model Improvement Plan, Attachment C3-2: Marsh Edge Erosion*. Version Final. (pp. 1-51). Baton Rouge, Louisiana: Coastal Protection and Restoration Authority.

Acknowledgements

This document was developed as part of a broader Model Improvement Plan in support of the 2017 Coastal Master Plan under the guidance of the Modeling Decision Team (MDT):

- The Water Institute of the Gulf - Ehab Meselhe, Alaina Grace, and Denise Reed
- Coastal Protection and Restoration Authority (CPRA) of Louisiana - Mandy Green, Angelina Freeman, and David Lindquist

The following experts were responsible for the preparatin of this document:

- John Atkinson - Arcadis, Inc.
- Hugh Roberts - Arcadis, Inc
- Dr. Ioannis Georgiou - University of New Orleans

This effort was funded by CPRA of Louisiana under Cooperative Endeavor Agreement Number 2503-12-58, Task Order No. 03.

Executive Summary

The erosion of marsh edges is a significant known mechanism for wetland loss in Louisiana. Consequently, the ability to simulate marsh edge erosion by wave action has been developed for inclusion in the 2017 Coastal Master Plan modeling effort. This addresses a knowledge gap identified in the 2012 Coastal Master Plan models. In addition to being able to project realistic wetland loss rates and locations along the coast, the model projections also estimate the sediment mass produced by a given retreat of the marsh edge, to pass to the Sediment Distribution subroutine of the 2017 Integrated Compartment Model (ICM). This requires an understanding of characteristic cross-shore bathymetry profiles and bulk density characteristics of coastal Louisiana wetland soils. In the context of this study, a compartment is a hydrologic unit consisting of open water, adjacent marsh, and attached upland area.

This report describes an investigation of the correlation between wave power and marsh edge retreat rates. Historical marsh edge change (derived from remote sensing data) and wave power (derived from wind records) along with marsh type, bulk density, and vegetation type were used in a multiple regression study. A coast wide selection of 1,343 points is used to derive regression relationships of marsh edge retreat rate versus wave power. Based on the literature, it was expected that these relationships could then predict future marsh edge retreat. However, the correlation coefficients were weak, and the comparisons of predicted and measured retreat rates show a very high scatter. It was concluded that the wave power regression equations were not adequate for coast wide predictions possibly due to the heterogeneity of the marsh-soil-sediment system and the simplicity of the wave interaction model. An alternative approach has been implemented in the ICM in which recent retreat rates were estimated from remote sensing data and then assigned as spatially variable edge erosion rates using a raster data set. These erosion rates are varied to account for project effects. Idealized marsh edge bathymetry is used to estimate sediment removal as a function of marsh edge retreat rate: a look-up table of sediment bulk density, organic content, and inorganic content can then be used to calculate mineral sediment yield from the retreat.

Table of Contents

List of Tables

List of Figures

List of Abbreviations

ADCIRC	ADvanced CIRCulation and Storm Surge model
AP	Airport
ASOS	Automated Surface Observation System
BD	Bulk Density
BS	Bankline Stabilization
CPRA	Coastal Protection and Restoration Authority
CRMS	Coastwide Reference Monitoring System
DEM	Digital Elevation Model
DOA	Date of Acquisition
FEMA	Federal Emergency Management Agency
GIS	Geographic Information System
GPS	Global Positioning System
ICM	Integrated Compartment Model
ISHD	Integrated Surface Hourly Database
MSY	New Orleans International Airport
NDBC	National Data Buoy Center
NCDC	National Climatic Data Center
NOAA	National Oceanic and Atmospheric Administration
OR	Oyster Reef
OWI	Ocean Weather Inc.
PBL	Planetary Boundary Layer
SAV	Submerged Aquatic Vegetation
SP	Shoreline Protection
USACE	United States Army Corps of Engineers
WAVCIS	WAVe-Current-Surge Information System

1.0 Introduction

In the State of Louisiana's 2012 Coastal Master Plan for coastal restoration and protection hundreds of restoration projects were modeled for 50 years into the future in an effort to identify high-performing projects(CPRA, 2012). CPRA is again utilizing modeling tools to support the 2017 Coastal Master Plan, building upon existing technical efforts where possible. In the 2017 analysis, individual project outcomes will again be assessed, but the focus will be on project interactions and sequencing. The models have been designed to efficiently run 50-year simulations with the ability to predict project effects at the basin-scale.

The overall vision for the 2017 analysis was to develop an ICM by building upon the technical tools used in the 2012 Coastal Master Plan, making revisions and improvements where possible, and developing entirely new tools in some instances. This report is the result of an expert subteam developing and testing a new process-based algorithm to include in the 2017 ICM for marsh edge erosion. The 2012 models did not simulate the erosion of marsh edges generated by wave action, despite this being a significant known mechanism for wetland loss in Louisiana (Penland et al., 2000; Day et al., 2000); edge erosion was only simulated when surface elevations dropped below mean sea level and the marsh was considered to be lost due to inundation. By not including this process in the 2012 models, shoreline protection projects were the only project type that demonstrated "restoration benefits" for reducing edge erosion, and the project effect on land loss was introduced through a "manual" adjustment of loss rates. Furthermore, eroded material was not considered a supply to the coastal system during previous modeling efforts. The focus of this work was to develop and test formulas to reflect key processes associated with marsh edge erosion and to develop a recommended approach for incorporation in the 2017 Coastal Master Plan modeling. In addition to projecting realistic marsh edge erosion rates at locations along the coast, the projections from this newly developed subroutine are also used to estimate the sediment mass produced by a given retreat of the shoreface-marsh scarp profile. This eroded sediment mass is used as a source term in other components of the ICM. This requires an understanding of characteristic cross-shore bathymetry profiles and bulk density characteristics of Louisiana wetland soils. The new marsh edge erosion subroutine is coded into the ICM.

The purpose of this document is as follows:

- To summarize the findings of a literature search on marsh edge erosion in coastal environments to provide guidance for the development of this component of the ICM
- To outline the coding necessary to implement the algorithm developed and tested in this phase
- To provide outcomes of the initial coding and testing
- To provide a robust alternative to the wave power density based regression equation

2.0 Literature Review

The first step of the subtask was to conduct a literature review of marsh edge erosion equations and modeling approaches. The review was conducted of relevant literature on marsh edge erosion, including both observational studies of relevant physical processes and numerical simulations of the process, from Louisiana and analogues elsewhere. This review identified a number of key issues and requirements that must be addressed to predict edge erosion rates at any open-water facing marsh edge. These issues are outlined below and are divided into those related to predicting erosion rates (i.e., erosion controls, Section 2.1), and those relating to determining mass yield per unit shoreline of a given linear erosion rate (i.e., yield controls, Section 2.2).

2.1 Erosion Controls

In previous studies, wave energy expended at the marsh scarp is the most utilized predictor of retreat rates (Marani et al., 2011; Trosclair, 2013). The key issue is to estimate wave energy along the shoreline. This calculation must include those variables that determine wave height and wave length, wave celerity, and ultimately, wave power (the wave energy flux per unit length of shoreline). These variables are controlled by factors that include wind speed and direction, open water fetch, and water depth over the fetch. Marani et al. (2011) provided an integrative model for explaining retreat rates using wave energy characteristics calibrated using retreat rates derived from remote sensing of Venice Lagoon, Italy. Marani et al. (2001) also tested the retreat-energy relationships that they developed in the Venice Lagoon against other global marsh edge regions (Figure 1). Trosclair (2013) utilized a simplified Marani approach for calculating wave energy characteristics (Young & Verhagen, 1996) and validated the Young and Verhagen wave equations as the most suitable for the shallow waters of coastal Louisiana. The Trosclair study involved field studies of wave and erosion rates in North Biloxi Marshes (Louisiana) and demonstrated that wave power calculated using this approach correlated well with the measured rate of retreat (Figure 2).

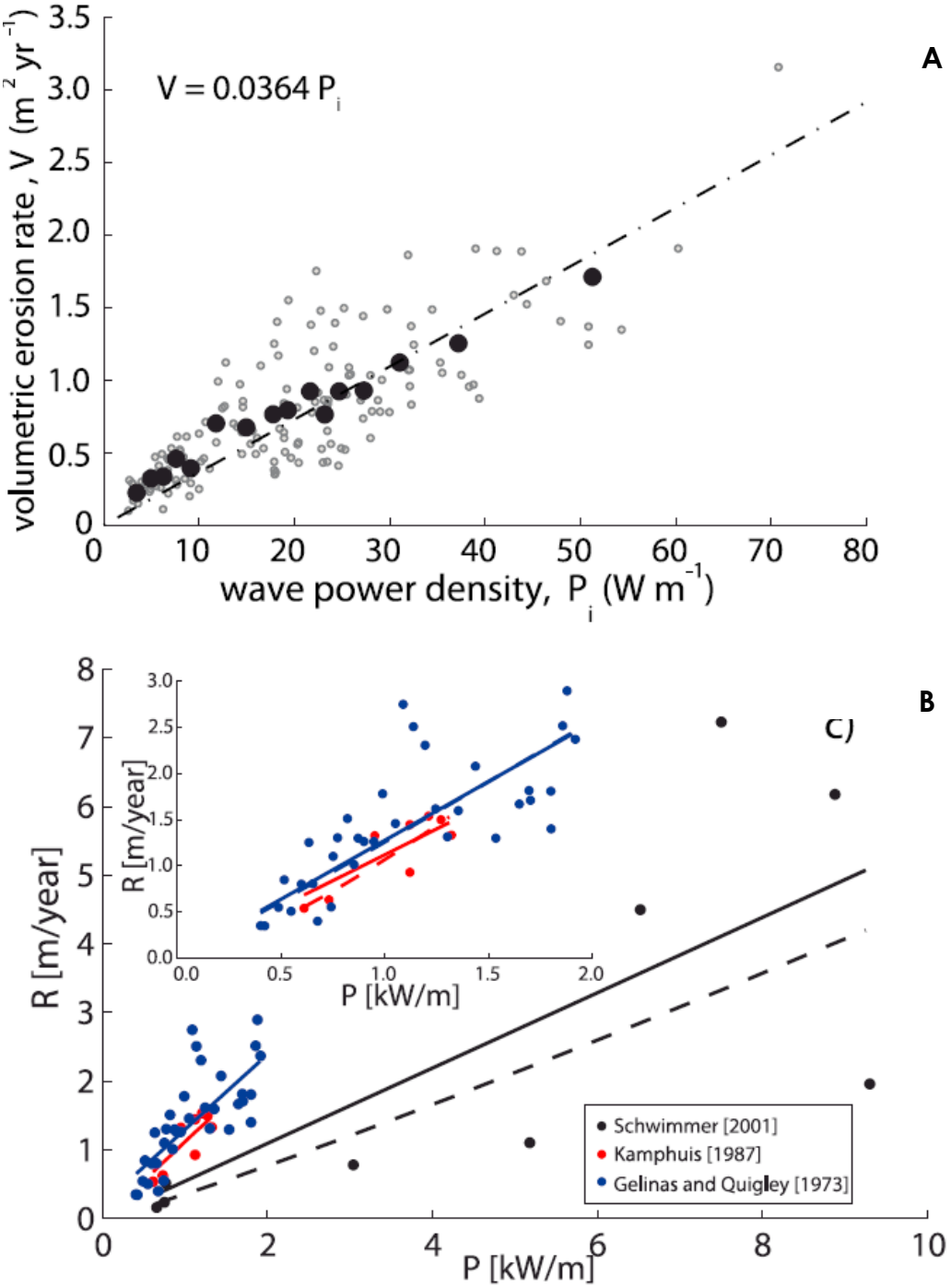

Figure 1: A. Wave power density and marsh edge erosion rate relationships for Venice Lagoon (Italy). These were developed using wave power calculated from wind data at 160 points around the lagoon and erosion rates from experimental data (e.g., flume measures of erosion rates from field samples taken at each site. Solid black circles indicate values obtained by averaging data over regular "bins" to emphasize overall trends. B. Summary of observations of wave power to edge erosion rate for other settings including glacial till (Gelinas & Quigley, 1973; Kamphuis, 1973) and Delaware Bay marshes (Schwimmer, 2001). Solid lines indicate the linear fits, while the dashed lines indicate the power law fits. The inset axes is an enlargement of the region closer to the origin. From Marani et al. (2011).

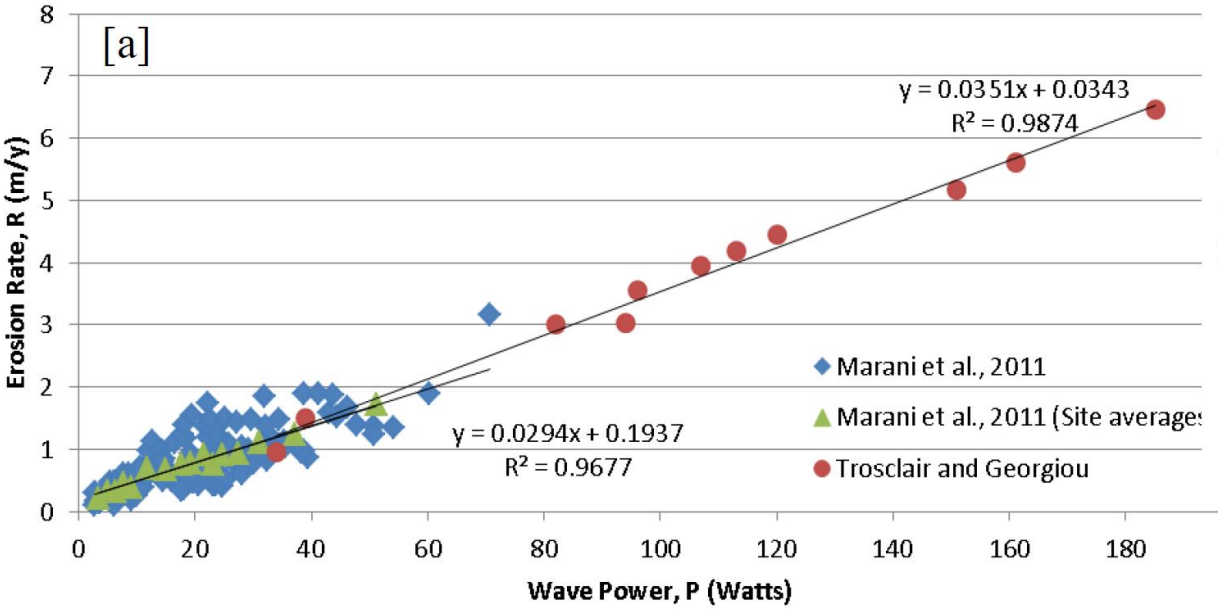

Figure 2: Marsh edge erosion rates for the Biloxi Marsh, Louisiana compared to Marani et al. (2011) in the Venice Lagoon (Italy). Graph shows good linear correlation between edge retreat and wave power (Trosclair, 2013).

The Young and Verhagen (1996) formula relationship utilizes fetch length, wind speed, and water depth to predict a wave height in finite water depth. The resultant wave characteristics can be converted to wave power using a method outlined in Marani et al. (2011) and corrected for orientation of wave direction relative to the marsh shoreline orientation. The wave power was computed from an annual wind rose for normal winds and 15-minute averaged winds for named storms. The detailed procedure is explained in Section 3.

Another impact on the wave energy that affects the marsh scarp is the potential wave damping effects of vegetation. While marsh vegetation can be neglected since it is landward of the marsh scarp, laboratory and numerical studies have shown that the effects of submerged aquatic vegetation (SAV) in the open water, over which waves are translating, are potentially significant (Augustin et al., 2009; Chen & Zhao, 2012; Jadhav et al., 2013). It was decided to ignore this effect because: 1) extent and character of SAV in coastal Louisiana is poorly documented, 2) this effect is likely species and density specific, and 3) the effect is likely too small in spatial scale to be able to generalize in the ICM marsh edge subroutine.

Waves may also erode bed sediments in the open water seaward of the marsh shoreface (e.g., the shoreface offshore limit taken where elevation goes asymptotic with bay bottom depths). While this process has been simulated in shallow basins (Fagherazzi & Wiberg, 2009) and is of importance to the sediment distribution subroutine being developed for the ICM, it is not considered in this marsh edge erosion model as it is considered to have a minor effect on the waves that cause inland translation of the marsh scarp (see Wilson & Allison, 2008 for a discussion of this bay bottom translation).

Whereas the process outlined by Marani et al. (2011) relates a wave energy calculation to marsh edge retreat rate, the shape of the cross-shore elevation profile, from the marsh scarp until it merges with the depths of the adjacent open water body, needs to be incorporated into this marsh edge erosion subroutine to help estimate sediment yields. The Wilson and Allison (2008)

study of Louisiana marsh edges measured the shoreface profile shape across multiple marsh edges in the Barataria and Breton Sound basins (Figure 3) and determined that the marsh shoreface profile was relatively consistent spatially and could fit an exponential decay with the equation:

$$y = -1.5 + 1.2e^{-0.05x} \quad (1)$$

Where y = distance offshore from marsh edge defined by the vegetation (m) and x = elevation relative to the marsh surface (in meters; Figure 3). Given the relatively wide spatial applicability of this exponential relationship and its source (i.e., from coastal Louisiana marshes), this equation was selected in the suggested path forward to represent a shape that will be translated shoreward with marsh erosion. Its wide spatial application provides some support for the assumption that the relationship will hold as edges retreat and marsh/open water surfaces change in relative elevation. Assuming a bulk density, the resulting loss volume can be converted to sediment mass released by the erosion. This will be used in the sediment distribution subroutine in the 2017 ICM. This process is described in detail in Section 3.

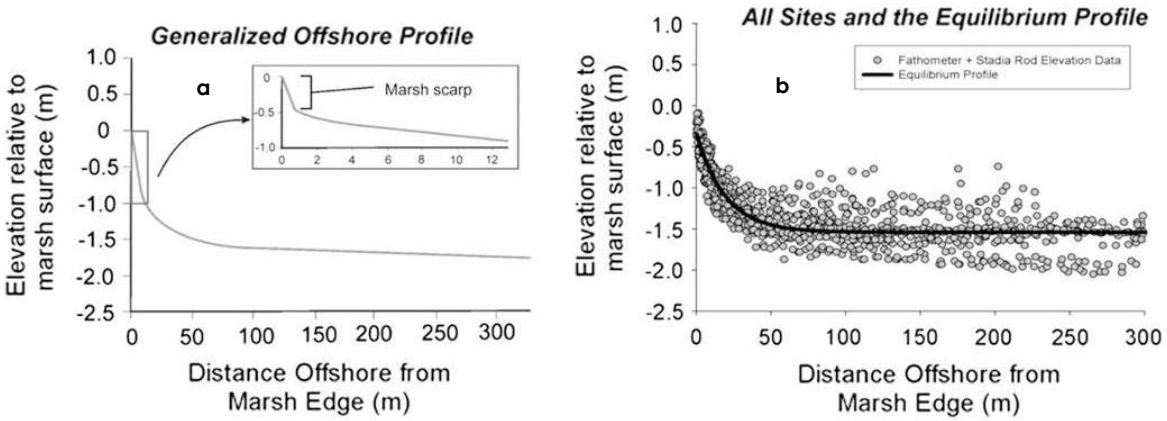

Figure 3: Diagram of (a) generalized offshore profile found in most Louisiana coastal marshes and (b) equilibrium profile (Equation 1) produced by all fathometer transects and transit measurements. From Wilson and Allison (2008).

For context to the processes described in this section and the preceeding section, Mariotti and Fagherazzi (2010) developed an integrated marsh-basin evolution model that includes marsh scarping and retreat, as well as remobilization and redistribution of sediments. This model captures retreat of marsh edge integrated over the entire shoreface, thus capturing in a numerical model the evolution described by the empirical shoreface profile from Wilson and Allison (2008).

The elevation of the marsh scarp is a factor in how wave energy is expended at the shoreline and how storm surge events submerge the marsh scarp, limiting direct wave breaking onto the marsh face (Trosclair, 2013). Relative sea level rise (eustatic sea level rise + subsidence) can cause the retreat of marsh shorelines independent of wave-induced processes by reducing elevation below the threshold for marsh survival. How should this marsh edge loss phenomenon be differentiated in the model development datasets? Subsidence rates are applied in the master plan models as a contributor to future elevation of existing marshes and open water areas. While subsidence is thus an additional factor influencing retreat rates, the loss of marsh due to decreased elevation is captured in other model subroutines.

Another unknown from the Louisiana wetland literature is whether the elevation of the marsh edge is specific to certain marsh types (e.g., fresh versus intermediate, etc.). While numerical modeling attempts have been made to simulate the effect of wave action on marsh boundaries as a function of tidal elevation and wave height for different edge configurations (e.g., Tonelli et al., 2010) and to identify individual processes acting at the marsh face (e.g., Francalanci et al., 2013), it was decided to omit this from the estimation of wave power expended at the shoreline.

In part, this is because on the Louisiana coast, water elevation changes due to typical astronomic tides and non-hurricane meteorological events are relatively small (i.e., generally less than 1 m, micro-tidal estuaries). This means that extreme submergence of the scarp or waves breaking landward of the scarp occurs only during a limited portion of the annually averaged wave power. Omitting the elevation of the water level relative to the marsh scarp elevation may not be valid for hurricane conditions. In these larger surges, the marsh scarp may be submerged by up to several meters of water, which may protect the scarp from wave attack (see discussion in Trosclair, 2013). Because of: 1) the relatively short period of hurricane impact (generally less than one week), and 2) the relatively large wave height in these events, applying the full period of hurricane waves to the wave power calculation can potentially have a disproportionate impact on the overall wave power expended at a site. Incorporating the effects of historical and future storms into predictions of marsh edge erosion, especially those that incorporate histroical data, is especially challenging due to the inherent inability to predict the exact magnitide and location of strom effects.

After predicting wave power that arrives at the shoreline, the other primary issue is how to convert wave power into a marsh edge erosion rate. It was decided to follow a modified version of the Marani calibration strategy (Figures 1 and 2) by utilizing historical erosion rates during a set period (2004-2012) at points across the coast to develop a set of calibration curves (for various wetland types and sediment properties such as bulk density or organic content) where wave power versus retreat can be calculated. More details are provided in Section 3. These curves could then be applied within the 2017 Coastal Master Plan ICM, requiring only simulated future wind statistics, water depth, and wave power to predict marsh edge retreat rates.

Watzke (2004) provides some precedent for applying a historical calibration based on wave power to determine future retreat rates in Louisiana wetlands. The Watzke study monitored a marsh island in northern Terrebonne Bay to determine changing elevation and the degree of marsh edge erosion over a period from 1999 to 2004. A nearby *Wave-Current-Surge Information System for Coastal Louisiana* (WAVCIS) station in Terrebonne Bay was utilized for wind wave statistics, as was a temporary station that measured wave height, water level, and temperature on the bay-facing and inland-facing faces of the island. Results provided calculations of marsh edge erosion (displacement distances) per month grouped into summer and winter conditions. Some statistics for loss in individual tropical storms were also presented. Wave statistics were compiled for several year averages by seasonal and both pre- and post- passage of winter cold fronts at the shoreline versus the open bay. The overall results of the study indicated a close relationship between wave statistics and marsh edge retreat. It should be noted that the marsh edge response was specific to an area where the upper, living root layer is underlain by a mineral rich strata (5% organic matter), a higher mineral content than most areas in coastal Louisiana.

The wave-stilling effects of biological structures (e.g., oyster beds and SAV beds) on the adjacent marsh shoreline may also be important. Although they may be significant, the relatively incomplete spatial knowledge of their extent and the poor quantification to date of

their wave-stilling effects in Louisiana or similar areas mean they are difficult to include specifically in a modeling approach.

What is the effect of large waves associated with tropical storm events? A number of past studies have concluded that hurricanes can have a major impact on marsh edge retreat relative to typical frontal storm rates. Morton and Barras (2011) provided a comprehensive descriptive survey of the effects of hurricanes – both depositional and erosional – on marsh surfaces in coastal Louisiana. In the survey of erosional mechanisms, it was found that some edges are capable of being modeled in the marsh edge subroutine of the ICM (e.g., shoreline erosion, pond expansion), while other situations are difficult to model (e.g., elongate pond formations, channelization, deformation due to longshore transport, and surface plucking). The study also provides some scale of erosion in individual events to potentially calibrate (10 - 160 m of shoreline translation) and describes individual storm impacts dating back to Hurricane Audrey (1957). Morton and Barras (2011) also provide descriptive differential impacts of low and high salinity marshes and low and high organic content marshes. The literature for individual events cataloged here could be utilized to calibrate a hurricane event impact. These storm catalogs could also be utilized to determine a minimum size for interior ponds before expansion would be considered in the 2017 Coastal Master Plan ICM. Palaseanu–Lovejoy et al. (2013) provide an examination of more recent events: a comparative remote sensing study of the effects of Hurricanes Katrina/Gustav (eastern coastal Louisiana) and Hurricanes Rita/Ike (western coastal Louisiana) using high resolution (e.g., Quickbird) imagery. Higher resolution imagery and improved classification of mixed land-water pixels allows better clarity of the processes that the master plan modeling effort is attempting to capture. This study also provides some comparison of effects on different marsh types.

2.2 Yield Controls

The bulk properties of Louisiana wetlands are a control on the erodibility of the marsh face and on the mass of mineral and organic particulate matter yielded. What are spatial patterns relative to mineral versus organic content and age/thickness of the marsh substrate layer, and how does it contribute to the retreat rate? Pant (2013) measured critical shear stress for two Louisiana coastal marshes – both the platform and marsh scarp – in Terrebonne Bay (Cocodrie) and Barataria Bay (Bay Jimmy) using a cohesive strength meter. Strength information coupled with time-series measurements of wave power can be used to determine the periods (when bottom shear stress exceeds sediment strength) from the forcing model when a specific marsh face is actively eroding. However, these measurements to date have only been conducted in a limited range of marsh types and locations in coastal Louisiana and may not account for all of the contributing factors (e.g., water level, the role of roots, etc.) Grabowski et al. (2011) identified all the variables that control the erodability of muddy (i.e., cohesive) sediments: physical, geochemical, and biological. The Grabowski dataset and description, while non-specific to Louisiana wetlands, is important for: 1) providing a general understanding of the limits of geotechnical impact on marsh edge erosion, and 2) guiding the process simplifications that can be realistically imposed in the eventual marsh edge subroutine model code.

Geotechnical properties of Louisiana wetlands related to dominant plant species (*Spartina*, etc.) could link – through root volume and depth – to erodibility of the marsh face. Howes et al. (2010) provide shear strength measurements, with depth through the marsh stratigraphy, comparing low and high salinity marshes in upper Breton Sound and their differential response to Hurricane Katrina, and finding a relationship between marsh type grouped by salinity that they attribute to geotechnical differences. Feagin et al. (2009) utilize field observations and laboratory flume studies to suggest that vegetation has a minor role in sufficiently binding sediment to impact wave erosion at marsh edges. They suggest that bulk density has the strongest control on rates

of shoreline retreat. They admit that vegetation may indirectly influence bulk properties increasing porosity through rooting, and by contributing organic content to the soils, which increases water content and increases erosion rates. All wetlands studied in Feagin et al. (2009) were in the Galveston Bay, Texas system. The results of the Galveston study suggest the possibility of simplifying physical properties of strength in the marsh edge ICM subroutine to a single parameter (i.e., bulk density) that encompasses variability induced by varying organic content and grain size.

Bio-erosion of marsh faces by burrowing and foraging fauna (e.g., infauna, Nutria, etc.) may also be a significant contributor to retreat of the marsh shoreface. Grabowski et al. (2011) outlines the possible mechanisms involved in bio-erosion, but there is insufficient information about its spatial and temporal impact on marsh edges in Louisiana to identify its role. It is also not clear that restoration projects proposed in the 2012 and 2017 master plans would influence these bio-erosion processes; inclusion of these processes would likely have little to no impact when evaluating the impact of proposed restoration projects.

Most of the literature research is for sites that are relatively homogenous in terms of soil and root zone characteristics. Although the correlation between marsh edge retreat and wave power density is very good in site specific cases, a more detailed description of the heterogenous marsh characteristics is needed for a coast wide model.

Given the factors mentioned above, estimation of sediment yield per unit shoreline for a given retreat rate could be related to the bulk properties of typical marsh substrates, and yield may include mineral particulates and particulate organic matter. One limitation for this modeling is that even if the database is available for current conditions it does not allow for how these properties will change in the future. Modeling thus has to assume that either there will be little future change, or that other ICM components will be able to predict this change. Given its potential for particle breakup or remineralization, and hence an assumed lesser importance in transport and deposition to increase elevation after release from the marsh edge, including the organic matter particulates in the yield may be unnecessary for this type of modeling, and considering mineral particles is more important. This information is available for all marsh types (U.S. Geological Survey National Wetlands Research Center database) in southern Louisiana.

2.3 Possible Modeling Approaches

Based on the evaluation of other studies, two approaches were identified as potentially viable to support estimation of marsh edge erosion and associated sediment yield in the ICM:

- Generation of edge erosion rates and sediment yield based on wind wave conditions in the adjacent water bodies, with rates varying over time due to changing winds, wetland-water configuration, and vegetation cover.
- Application of historical edge erosion rates for specific water bodies/shorelines with erosion remaining constant over time and sediment yield varying according to changes in marsh soil type in accordance with changes in vegetation cover.

Both of these require the acquisition of data and consideration of the specific configuration of the Louisiana coast and the locations where marsh erosion is most important.

3.0 Time Varying Edge Erosion Data and Analysis

This approach involves retrieving wind speeds and directions, fetch, depth, and marsh retreat directions and using them to calculate the average wave power for each marsh edge location (Figure 4). A regression relationship between marsh retreat rate (as determined from aerial imagery) and average wave power can then be determined for each marsh type grouping, where the groupings are determined by variation in processes (e.g., erodibility of different soil types) and can be supported by the regression analysis. The regression coefficients are used with the calculated wave power to estimate the retreat rate for each marsh edge location included in the ICM. The sources and dates for the imagery are described in section 4.

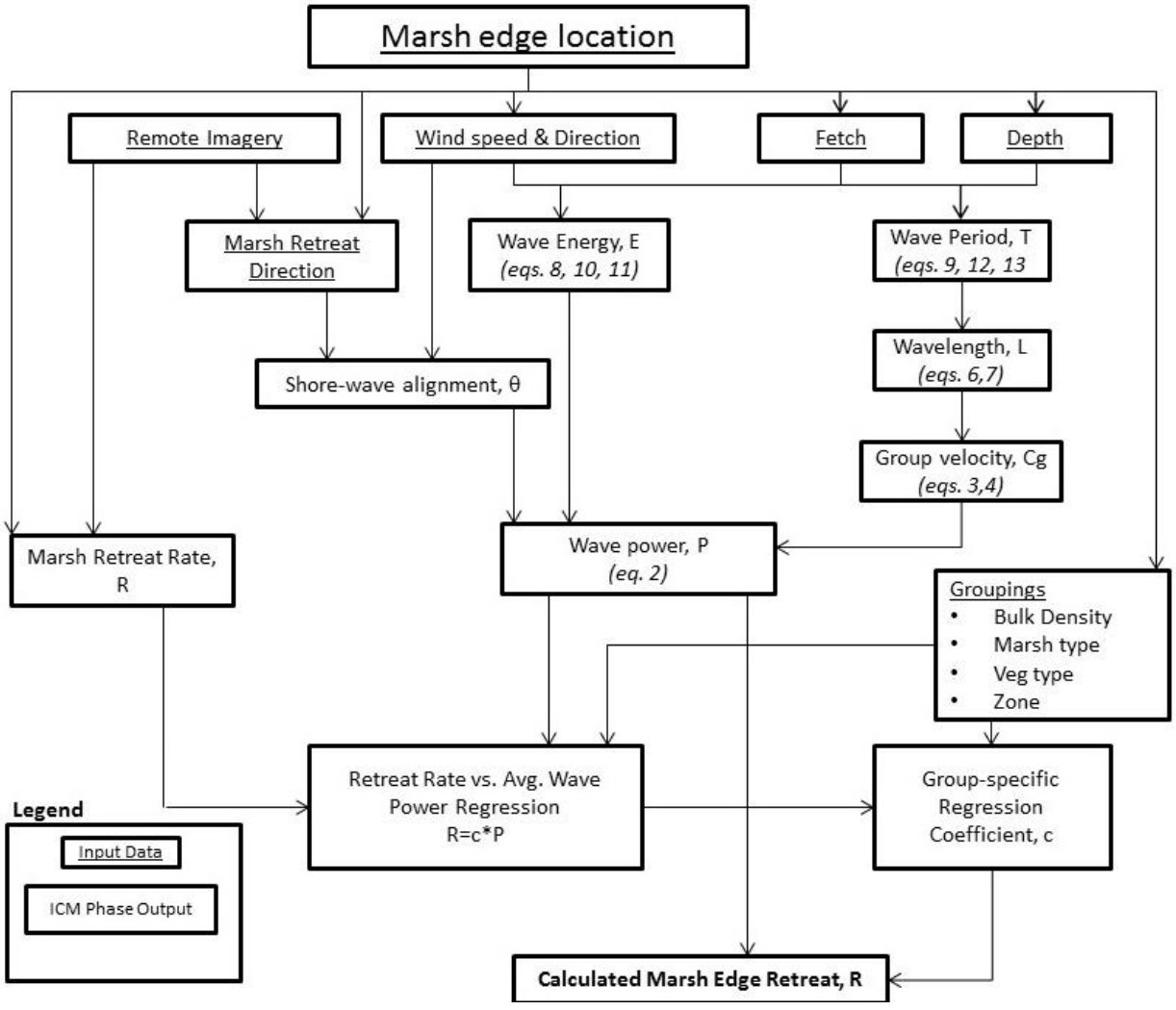

Figure 4: Overall process diagram used in the time varying marsh edge erosion approach.

3.1 Wind Statistics Applied to the Wave Power Calculations

The objective of this step in the model development phase was to:

- Collect available wind station data across Louisiana;
- Process the wind data to a common temporal, height, and direction/speed datum;
- Select stations to subdivide the coastal areas in areas where a single station's data would be applied to the wave power calculation.

The defining criteria utilized to select specific stations were to:

- Require both wind speed and direction data that was needed for the wave power equation;
- Select stations representative of coastal Louisiana basins (Table 1 and Figure 4);
- Extend data collection to at least over the time period of 2004-2012 to coincide with available aerial imagery (see section 4);
- Identify currently active stations (e.g., post-2012) for potential use in future model runs;
- Undertake continuous data collection at a subhourly sampling frequency that can be utilized to generate appropriately time-averaged wind statistics; the averaging unit must be long enough to average out gusts and meet fetch-limited wave duration requirements;
- Obtain metadata that allow for comparison of how wind data were collected and reported to enable comparisons and reduce bias.

Stations were selected if the above criteria were met and were rejected otherwise (Tables 1 and 2).

Three different datasets were examined, each at different timescale resolutions:

- 2-minute average on the hour (NDBC and ASOS)
- 10-minute average 6 times per hour (NDBC)
- 1-minute average (ASOS)

3.1.1 2-Minute/Hour Data

The 2-minute hourly dataset was retrieved from the Integrated Surface Hourly Database (ISHD) from the National Climatic Data Center (NCDC), which provides quality controlled hourly data for both airport and coastal stations: Sabine, Lake Charles AP, New Iberia AP, Grand Isle, Southwest Pass, New Orleans AP (see Table 1 for station information). Both the Automated Surface Observation System (ASOS) and National Data Buoy Center (NDBC) report wind velocity and direction for these stations using comparable measuring and averaging methods. The NDBC reports wind speed and direction averaged over two minutes on the hour, which are reported hourly. ASOS reports an hourly value that is calculated during the first 2-minute average of the hour, using a 5-second running average to derive the 2-minute average. The ISHD reports wind direction to the nearest 10th degree. Collection and processing methods are consistent across stations. However, the data contain spikes because the hourly 2-minute sampling is not as representative as sampling over an entire hour. Stations used are shown in Table 2.

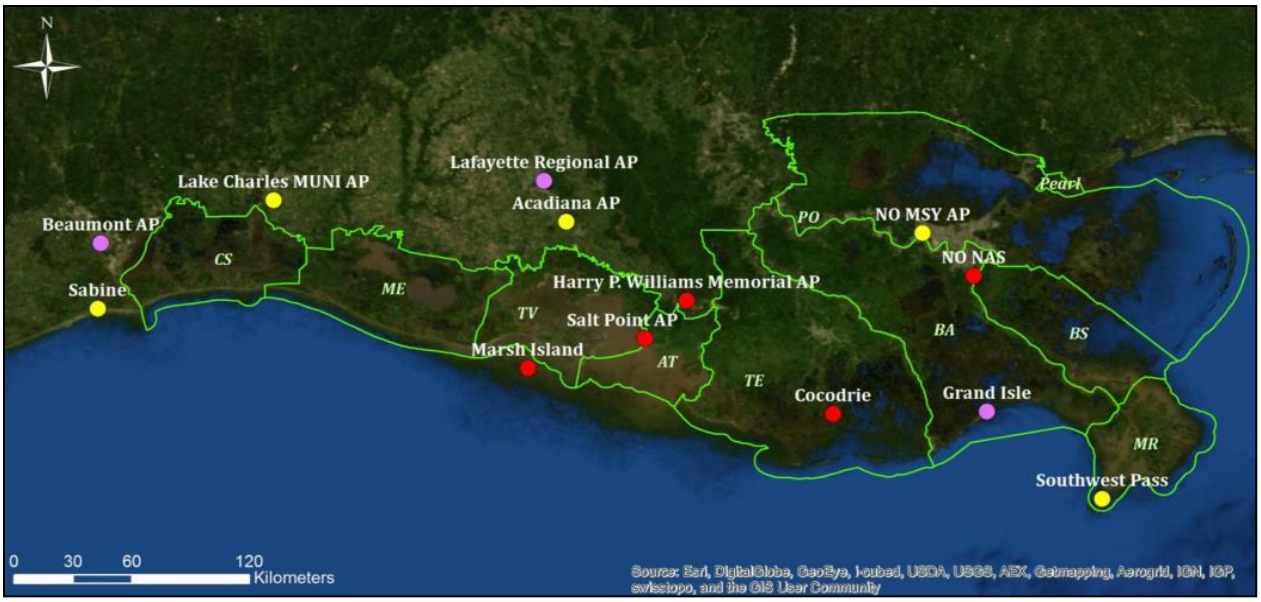

→ **Red stations:** did not meet criteria and/or incomplete dataset and/or unavailable station information
→ **Yellow stations:** 10 minute data throughout the hour
→ **Violet + Yellow stations:** 2 minute data on the hour

Figure 5: Wind stations identified for potential inclusion in the wave power calculations.

Table 1: Wind stations considered and station information.

Station Name	Station Type	Station Owner	USAF ID	LAT	LONG	Site Elevation (m above MSL)	Anemometer (m above site)	Reason Rejected
Grand Isle*	C-MAN	NDBC	994290	29.267 N	89.957 W	1.8	15.8	No continuous winds and many data gaps
Grand Isle*	CO-OPS	NOS	994977	29.263 N	89.957 W	2.7	6.5	
Lake Charles MUNI AP	ASOS	NWS-FAA	722400	30.125 N	93.228 W	2.7	10.1	
Lafayette Regional AP	ASOS	NWS-FAA	722405	30.205 N	91.988 W	12.8	7.9	
Marsh Island	Shore-based tower	CSI LSU	997236	29.440 N	92.061 W	0.0	23.4	
Acadiana AP*	ASOS	NWS-FAA	722314	30.033 N	91.883 W	7.0	7.9	
Acadiana AP*	ASOS	NWS-FAA	722314	30.038 N	91.884 W	7.3	7.9	
NO MSY AP	ASOS	NWS-FAA	722310	29.993 N	90.251 W	6.1	10.1	

Station Name	Station Type	Station Owner	USAF ID	LAT	LONG	Site Elevation (m above MSL)	Anemometer (m above site)	Reason Rejected
NO NAS JRB	N/A	Private	722316	29.817 N	90.017 W	0.3	-	Cannot obtain metadata
Beaumont AP	ASOS	NWS-FAA	722410	29.951 N	94.021 W	4.9	10.1	Already have Lake Charles AP for SW LA
Sabine	C-MAN	NDBC	994260	29.683 N	94.033 W	0.7	9.1	
Southwest Pass	C-MAN	NDBC	994010	28.905 N	89.428 W	0.0	30.5	
Cocodrie	Shore-based tower	LUMCON	994780	29.253 N	90.663 W	0.0	13.2	Cannot obtain metadata and many data gaps
Harry P. Williams Memorial AP	AWOS III	FAA	722329	29.717 N	91.333 W	2.7	-	No metadata for AWOS III station type
Salt Point*	ASOS	NWS-FAA	722403	29.560 N	91.533 W	0.0	10.1	Many data gaps, especially 2004-2005
Salt Point*	ASOS	NWS-FAA	722404	29.562 N	91.526 W	0.6	10.1	

(*) indicates stations that were moved during time interval of interest.

3.1.2 10-Minute Data

Higher resolution data are also available for both the coastal and airport stations. The NDBC has a limited number of stations that report continuous winds data, which are a 10-minute average every 10 minutes throughout the hour (Table 2). The two coastal stations with continuous winds data are Sabine and Southwest Pass. The averaging algorithm uses a scalar average for wind speed and a unit vector average for the wind direction.

3.1.3 1-Minute Data

The ASOS airport stations also report 1-minute averaged data. The three airport (AP) stations that meet criteria and were examined for this exercise are Lake Charles, New Iberia (Acadiana), New Orleans (MSY).

It was decided to average the 1-minute dataset using the same methods as the NDBC averaging methods to make the datasets consistent with the continuous winds 10-minute data and to smooth wind gusts in the dataset. It was also decided to add the Marsh Island station, which has hourly 10-minute averages, in order to fill in the central coastal Louisiana spatial gap

and obtain a more complete coverage. Though the collection methods are different at this station, wind information from central coastal Louisiana is required to represent the diverse coastline.

Table 2: Data inventory of full date range excluding hurricane days for both the 2-minute and 10-minute datasets.

Station	# 2 Min Hourly Data[1]	% Complete	# 10 Min Data	% Complete
Beaumont AP	66,065	84.6		
Grand Isle	59,802	76.6		
Lafayette AP	53,425	68.4		
Lake Charles AP	61,183	78.4	435,445	93.0
New Iberia AP	61,395	78.6	380,836	81.3
New Orleans AP	65,625	84.1	437,522	93.4
Sabine	71,724	91.9	436,117	93.1
Southwest Pass	51,821	66.4	318,012	67.9

3.2 Data Processing

For all data processing, blanks and duplicates were removed and all wind speeds were converted to m/s. Normal wind data that coincided within the week centered on one of the five major hurricane landfall dates during this time period were also removed for the periods:

- 08/26/2005 – 09/01/2005: *Katrina(150 Kt)*
- 09/21/2005 – 09/27/2005: *Rita*
- 08/28/2008 – 09/03/2008: *Gustav(135 Kt)*
- 09/10/2008 – 09/16/2008: *Ike* (125 Kt)
- 08/25/2012 – 08/31/2012: *Isaac (70 Kt)*

The purpose of this removal was to improve a site's record with station specific winds using the Ocean Weather Inc. (OWI) wind fields as described in Section 3.3. All stations encompass the time period 01/01/2004–12/31/2012. However, a few stations with large data gaps (Tables 2 and 3) were identified, notably, Sabine, New Iberia AP, and Southwest Pass.

[1] Note that a complete 9 year record would include 78,072 records for 10 minute data and 468,432 records for 2 minute data

Table 3: Data inventory of imagery date ranges for the 10-minute dataset.

Station	Start	End	# Data	% Complete
Date range 1 (Katrina & Rita)	**1/19/2004**	**10/27/2005**	**91296**	
Lake Charles AP	1/19/2004	10/27/2005	83234	91.2
New Iberia AP	3/3/2005	10/27/2005	28333	31.0
New Orleans AP	1/19/2004	10/27/2005	83525	91.5
Sabine	1/19/2004	10/27/2005	90996	99.7
Southwest Pass	1/19/2004	8/25/2005	83959	92.0
Date range 2 (Gustav & Ike)	**10/28/2005**	**10/29/2008**	**156096**	
Lake Charles AP	10/28/2005	10/29/2008	144818	92.8
New Iberia AP	10/28/2005	10/29/2008	144760	92.7
New Orleans AP	10/28/2005	10/29/2008	145231	93.0
Sabine	10/28/2005	9/9/2008	147589	94.6
Southwest Pass	12/21/2005	8/30/2007	87422	56.0
Date range 3 (Isaac)	**10/30/2008**	**11/14/2012**	**211680**	
Lake Charles AP	10/30/2008	11/14/2012	198312	93.7
New Iberia AP	10/30/2008	11/14/2012	201121	95.0
New Orleans AP	10/30/2008	11/14/2012	199838	94.4
Sabine	4/9/2009	11/14/2012	188177	88.9
Southwest Pass	8/23/2009	4/4/2012	137403	64.9

In general, tropical storms were not removed from the normal wind rose since it was assumed that they are not extremes and are represented by the low frequency bins of the normal wind rose associated with a specific marsh edge point. Since the mean depth is used in the wave power computations, the storm surge is not included for any of the computations. This could lead to an under-estimation of the wave power density since in some locations the waves are depth limited. For example, in 2011 the Tropical Storm Lee surge in Terrebonne Bay was measured to be about 1 m; this would produce higher wave power due to the greater mean depth and the higher local wind speeds compared to the wind rose. Ideally, a better spatial description of the wind field and the associated water depth along the fetch would give improved estimates of the wave power; however, since the durations of these storms is relatively short, the impact on the average annual wave power density at a local site is of the order of 50% greater which is not sufficient to explain the large scatter (orders of magnitude) in the observed retreat rates compared to the erosion-wave power based predictions. The following tropical storms have been represented in the normal wind rose:

- 10/10-11/2004: Tropical Storm Matthew (40 Kt, Max. sustained winds at landfall)
- 8/15-26/2008: Tropical Storm Edouard (55 Kt)
- 11/4-10/2009: Tropical Storm Ida (90 Kt)
- 7/22-24/2010: Tropical Storm Bonnie (40 Kt)
- 9/2-5/2011: Tropical Storm Lee (50 Kt)

Data post-processing utilized the methods described below.

3.2.1 Wind Power Law Method

Station elevation and anemometer elevations were retrieved from the NDBC and the ASOS. Anemometer elevation information was used to standardize wind velocity at 10 m according to the Power Law Method as described by Hsu et al. (1994): $u_2 = u_1 (z_2/z_1)^P$, where P = 0.11. Most airport station anemometers are already set at 10 m above the surface. The NDBC and airport anemometers that are not at 10 m have been adjusted using the Power Law Method.

3.2.2 Averaging

The ASOS 1-minute dataset was averaged to 10 minutes using the same method as the NDBC. The wind speed uses a scalar average. The wind direction uses a unit vector average. Each wind direction observation is converted to radians, after which the u and v vectors are derived. Then, the u and v vectors are averaged to a 10-minute vector average. Next, the wind direction is calculated from "arctan (u/v)," which is then converted back to degrees.

What is finally reported is the frequency of the median wind speed and direction, rather than the average, in order to avoid misrepresentation from extreme high winds. The median wind direction and speed were determined using the date intervals described above and wind direction and speed bins.

3.2.3 Wind Direction

The wind direction quadrant hourly data are divided into 16 directions at 22.5° intervals.

Here is an example of the NE quadrant:

- 348.75° - 11.25° (N)
- 11.25° - 33.75° (NNE)
- 33.75° - 56-25° (NE)
- 56.25° - 78.75° (ENE)
- 78.75° - 101.25° (E)

3.2.4 Wind Speed

The wind speed hourly data are divided into nine bins using the Beaufort Scale, which is a standard meteorological and oceanographic categorization of wind speed.

- In m/s: Calm <1, 1-2, 2-3, 3-5, 5-8, 8-11, 11-14, 14-17, storms >=17

3.2.5 Missing Data

Missing data were processed by averaging all available data for a given time-step and station and using that average value for the data in the missing time-step for that station. All such values are flagged. Southwest Pass does not have any data available for 2008; therefore, that year for this station is excluded from the dataset. Missing data for all stations, except Southwest Pass, were smaller and are the result of many small discontinuous gaps; further, these datasets are 88% complete or greater (Table 2). Therefore, an average value for a given missing time-step was used and deemed appropriate. The missing data for 2008 for Southwest Pass resulted in less

than a 60% complete dataset (Table 3, Date 2). For this reason, using an average value to complete 2008 would have misrepresented the wind data at that station for that year.

Figure 6 shows an example of a wind rose generated from the New Orleans airport 1-minute dataset averaged to the hour to fit within the limits of the wind rose plotting software (WRPLOT View from Lakes Environmental).

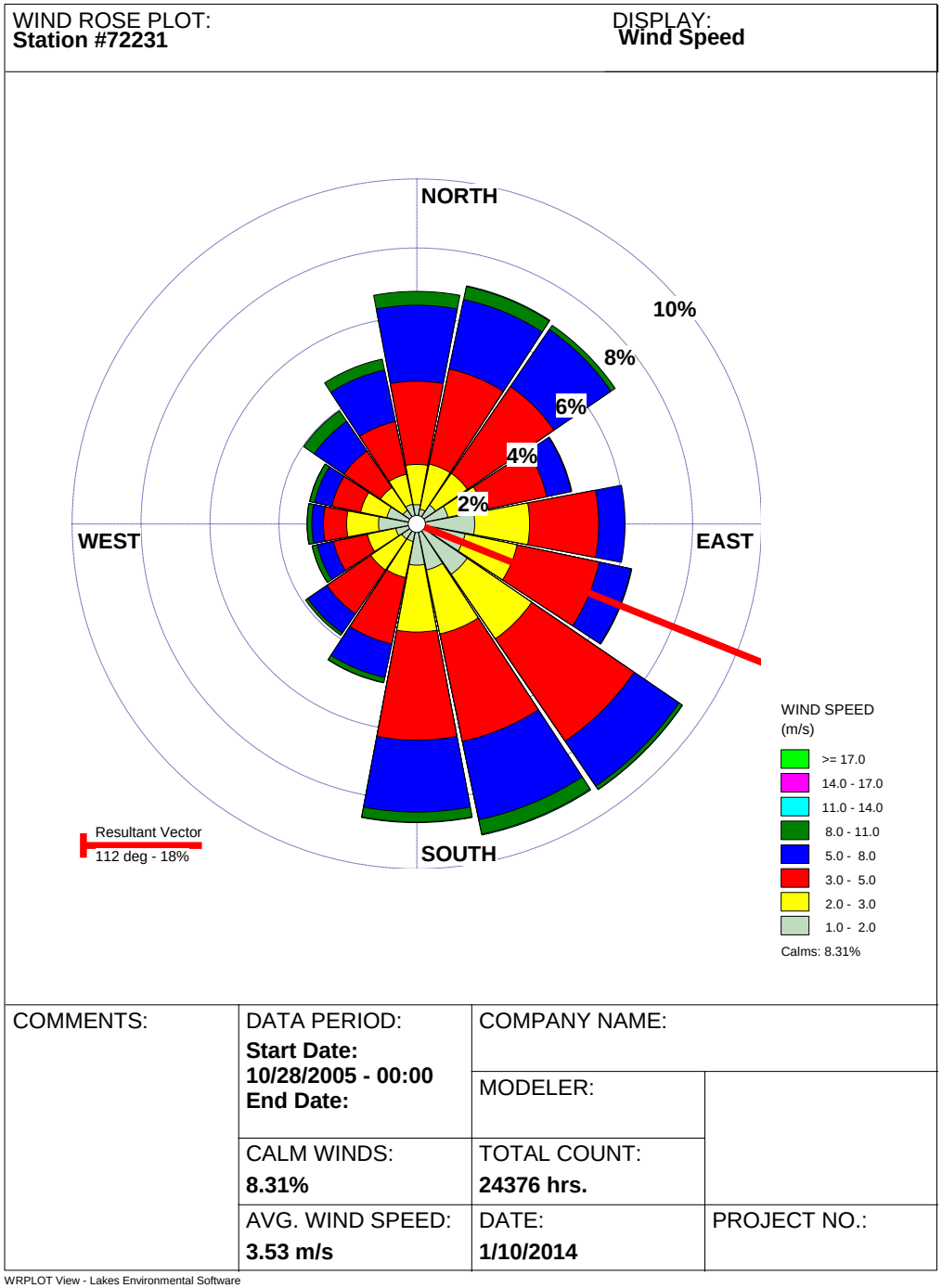

Figure 6: Example wind rose generated from New Orleans airport 1-minute ASOS data averaged to 10 minutes (and then hourly for the wind rose plotting program) during the 2005-2008 image date interval.

3.3 Use of Wind Observations in Wave Power Computations

Wind observations across coastal Louisiana were used to develop wind roses for the same time intervals as the available satellite imagery. Each wind rose was developed for nine wind speed Beaufort Scale ranges, *s*, and 16 directional sectors, *dir*. Each wind rose consisted of the number of wind observations within each speed range and directional sector, $n_{dir,s}$, divided by the total number of wind observations, n_{obs}. The wind data were also analyzed to determine the median wind speed at a height of 10 meters for each speed range and directional sector, $U_{dir,s}$.

At each marsh edge transect location (see Section 4), fetch was calculated in each of the 16 directional sectors. The bathymetric database from CRMS described in section 4.0 was also used to calculate an average water depth based the tide filtered mean water level, *d*, along each of these fetches.

The average wave power acting upon a marsh edge location during non-storm conditions was calculated for each wind speed and direction combination provided in the wind rose, which has storm winds removed (Category 1 or higher). The wave power produced by each speed/direction combination was then weighted by the portion of wind observations that fell within that speed/direction range. The average wave power density acting upon a marsh edge is the sum of these weighted wave powers across the entire wind speed and direction field plus the average wave power contributed by storms (derived from the OWI wind statistics; see Section 3.1) during the same time period. Each of these two average wave powers is weighted by the proportion of time under either non-storm or storm conditions, as shown in Equation 2:

$$\bar{P} = \left[\sum_{dir=1}^{16}\sum_{s=1}^{9}\left(P_{dir,s}\frac{n_{dir,s}}{n_{obs}}\right)\right]\left(\frac{t_{nonstorm}}{t_{total}}\right) + \bar{P}_{storm}\left(\frac{t_{storm}}{t_{total}}\right) \quad (2)$$

where $\bar{P}$ is the average wave power density index acting upon a marsh edge, $P_{dir,s}$ is the wave power density index calculated for a wind direction and wind speed combination as summarized in the wind rose (denoted by the *dir* and *s* subscripts, respectively), $n_{dir,s}$ is the number of wind observations for a wind direction and speed combination provided in the wind rose, n_{obs} is the total number of wind observations used to develop the wind rose, $\bar{P}_{storm}$ is the average wave power density index from hurricanes, t_{total} is the total number of days for which marsh retreat was calculated (defined by the dates of the aerial imagery intervals), $t_{nonstorm}$ is the number of days within the imagery interval not defined as a hurricane period, and t_{storm} is the number of days within the interval considered to be hurricane conditions (see Section 3.1 for periods defined as hurricane conditions). A discussion of wave power calculations from storm periods follows in Section 3.3. Since the wave power density is based on two different temporal averaging procedures, the term 'index' is used to indicate the mixed integration intervals.

The following formulation is applicable to both the 'normal' wind and the storm wind periods (see Section 3.4). The wave power density (W/m), *P*, as required for Equation 2, is calculated as:

$$P_{dir,s} = C_{g_{dir,s}} E_{dir,s} \rho g \cos\theta \quad (3)$$

where C_g is the wave group velocity (m/s), *E* is the wave energy (m^2; specifically, the zeroth moment of the wave energy spectrum), ρ is density of water (kg/m^3), *g* is acceleration due to gravity (m/s^2) and θ is the angle between the wave direction and the direction of marsh retreat. It is assumed that marsh retreat will always be perpendicular to the marsh edge. Therefore, θ will equal 0° for waves that are moving perpendicular to the marsh edge and θ will equal 90° for waves moving parallel to the marsh edge, with only winds with an on-shore component considered.

From linear wave theory, group velocity, C_g, is calculated as:

$$C_{g_{dir,s}} = N_{dir,s}\frac{L_{dir,s}}{T_{dir,s}} \quad (4)$$

where *L* is wavelength (m), *T* is wave period (s), and *N* is calculated with Equation 5.

$$N_{dir,s} = 0.5\left(1 + \frac{4\pi d_{dir}/L_{dir,s}}{\sinh(4\pi d_{dir}/L_{dir,s})}\right) \quad (5)$$

Wavelength, *L*, can be iteratively solved from depth, *d*, and wave period, *T* (Equation 6).

$$L_{dir,s} = \frac{gT_{dir,s}{}^2}{2\pi}\tanh\left(\frac{2\pi d_{dir}}{L_{dir,s}}\right) \quad (6)$$

However, a reasonably accurate (±10%) noniterative approximation (Equations 7 and 8) for wavelength will be used for simplicity (Demirbilek & Vincent, 2002).

$$L_{dir,s} \approx L_o\sqrt{\tanh\left(\frac{2\pi d_{dir}}{L_o}\right)} \quad (7)$$

$$L_o = \frac{gT_{dir,s}{}^2}{2\pi} \quad (8)$$

Equations 3 through 8 require four input variables θ, *d*, *T,* and *E*, two of which, θ and *d*, are physical characteristics of the marsh location. Wave period and wave energy are derived using the Young and Verhagen (1996) wave model.

From fitting established wave spectrum equations to observed datasets and non-dimensional analysis, Young and Verhagen (1996) developed empirical relationships for wave energy, *E*, and wave period, *T* (or frequency, *V)*, from depth (m), *d*, fetch (m), *X*, and *U,*wind speed (m/s) at 10 m as described in Section 3.1. The Young andVerhagen equations are derived for fetch limited conditions; when the durations are insufficient to yield the fetch limited waves, an equivalent fetch should be used as discussed later.

$$E_{dir,s} = E_{lim}\left\{\tanh A_1 \tanh\left(\frac{B_1}{\tanh A_1}\right)\right\}^n\left(\frac{U_{dir,s}{}^2}{g}\right)^2 \quad (9)$$

$$\frac{1}{T_{dir,s}} = V_{dir,s} = V_{lim}\left\{\tanh A_2 \tanh\left(\frac{B_2}{\tanh A_2}\right)\right\}^m\left(\frac{g}{U_{dir,s}}\right) \quad (10)$$

where,

$$A_1 = 0.292^{1/n}\left[d_{dir}\frac{U_{dir,s}{}^2}{g}\right]^{1.3/n}\left[d_{dir}\frac{U_{dir,s}{}^2 g}{U_{dir,s}{}^2 g}\right]^{1.3/n} \quad (11)$$

$$B_1 = (4.396\times10^{-5})^{1/n}\left[X_{dir}\frac{U_{dir,s}{}^2}{g}\right]^{1/n}\left[X_{dir}\frac{g}{U_{dir,s}{}^2}\frac{U_{dir,s}{}^2}{g}\right]^{1/n} \quad (12)$$

$$A_2 = 1.505^{1/m}\left[d_{dir}\frac{U_{dir,s}{}^2}{g}\right]^{-0.375/m}\left[d_{dir}\frac{g}{U_{dir,s}{}^2}\frac{U_{dir,s}{}^2}{g}\right]^{-0.375/m} \quad (13)$$

$$B_2 = 16.391^{1/m}\left[X_{dir}\frac{U_{dir,s}{}^2}{g}\right]^{-0.27/m}\left[X_{dir}\frac{g}{U_{dir,s}{}^2}\frac{U_{dir,s}{}^2}{g}\right]^{-0.27/m} \quad (14)$$

Ongoing studies in the Biloxi Marsh, Louisiana(J.A. McCorquodale, per.comm.) indicate that coefficients and exponents originally proposed by Young and Verhagen for equations 9 through 14 produce acceptable results for water bodies in the Gulf Coast region: E_{lim}=0.00364, V_{lim}=0.133, n=1.74 and m=-0.37 (Trosclair, 2013; Filostrat, 2014).

The Young and Verhagen wave model is applicable to fetch-limited wave conditions, which require that the wind speed used in the above equations have been sustained for a long enough period to reach fetch-limited waves. The wave height is limited to the transitional wave breaking height of 78% of the depth. A process outlined in the Army Corps of Engineers' Coastal Engineering Manual (Resio et al., 2002) can be followed to ensure that fetch-limited conditions are met. The duration that the wind speed should be sustained to reach these conditions is determined by:

$$t_{req} = 77.23 \frac{X^{0.67}}{u_{10}{}^{0.34} g^{0.33}} \quad (15)$$

If the averaging interval used in the wind data is less than this required duration, t_{req}, an equivalent fetch, X_{eq} must be calculated and substituted for fetch, X, in the Young and Verhagen equations (Resio et al., 2002). The equivalent fetch is calculated from the time-step used to average the wind record, t_{dur}, and wind velocity at 10 m above the surface. u_{10}, is used to estimate a drag coefficient, C_D, and the friction velocity, u_*.

$$X_{eq} = 5.23 \times 10^{-3} \sqrt{t_{dur}{}^3 g u_*} \quad (16)$$

$$u_* = u_{10} \sqrt{C_D} \quad (17)$$

$$C_D = 0.001(1.1 + 0.035 u_{10}) \quad (18)$$

All wave power calculations and power-retreat correlations were completed within the *R* statistical computing environment (R Core Team, 2013). A brief discussion of the algorithms and the testing of the algorithms is provided in Section 4.

3.4 Tropical Storm Winds

OWI supplied wind data, prepared in support of previous Federal Emergency Management Agency (FEMA) and U.S. Army Corps of Engineers (USACE) projects, are available for the 1,343 marsh edge transect locations and were utilized in this wave power-retreat regression exercise for the five hurricane periods defined earlier (Katrina, Rita, Gustav, Ike, and Isaac). Rather than use a windrose format for hurricane periods, the process outlined in Section 3.3 (Equations 3 through 18), can be applied to a wind time-series at each of the 1,343 marsh edge transects during each of the five hurricanes. The wind speed and direction at each 15-minute time-step can be used to calculate a shore-normal wave power for each time-step. This results in a time-series of wave power calculations during each storm. These wave power time-series can then be averaged together to determine an average wave power per storm, which can be used in Equation 2 to determine the overall average wave power affecting each marsh edge transect for the various imagery date ranges.

The winds available from OWI are a combination of data assimilated wind snapshots from the H*Wind model (developed by the National Oceanographic and Atmospheric Administration ([NOAA]) and data from OWI's proprietary Planetary Boundary Layer (PBL) model. The H*Wind model assimilates all available observations of wind speed and direction during the storm,

composites these relative to the storm's center, and transforms them to a common 10 m height at full marine exposure (Powell & Houston, 1996; Powell et al., 1996, 1998). The H*Wind model produces snapshots of the storm conditions at hourly intervals, and the PBL model solves the governing equations for atmospheric flow within the planetary boundary layer. The hurricane's pressure field is defined by a parametric relationship (Holland, 1980). To provide forcing to t surge and wave modelsl, the H*Wind fields are blended with larger-scale PBL wind fields using the Interactive Objective Kinematic Analysis system (Cox et al., 1995; Cardone & Cox, 2007). The resulting wind fields reference the condition of 10 m height, 30 minute "sustained" wind speed, and full marine exposure. Wind fields were interpolated to 15 minute intervals.

Simulations of Hurricane Katrina, Rita, Gustav, and Ike were performed using the wind forcing described above. However, Hurricane Isaac wind data were developed solely from PBL model results; there was no data assimilation from the H*Wind model. Due to Isaacs's slow forward progress, it exhibited atypical winds, and is not well represented by the PBL model results. Even though the wind data for Isaac is known to be rather poor, it will be assumed (for this development phase), that the PBL wind data is still more representative of actual hurricane winds than the long-term average winds from the 5 wind stations used in this analysis, which is the alternative wind data source if the PBL wind data are discarded for Isaac.

4.0 Historical Rate Approach Data and Analysis

This approach entails a historical model development strategy based on an established relationship in the literature (e.g., Marani et al., 2011; Trosclair, 2013; Figures 1 and 2) between wave power and retreat rate of marsh scarps. This approach uses historic data on wetland retreat rates at various points across the Louisiana coastal zone, paired with wave power calculated for that location during the same historical interval.

To derive the wave power – marsh retreat rate calibration, the period 2004-2012 was selected because it has four (e.g., 2004, 2007, 2009, 2012) high-quality aerial overflight datasets of shoreline positions coast wide in Louisiana. These four imagery data sets yield three date ranges which can be used for comparing wave power and marsh edge retreat. Five hurricanes occurred during these date ranges (e.g., Katrina and Rita in date range 1 (2004-2007), Gustav and Ike (2008) in date range 2, etc.).

Wave power is calculated for each shoreline location using the Young and Verhagen (1996) formula that requires open water fetch, average water depth across the fetch length, and wind speed to determine the wave energy at the marsh edge. A total of 1,343 model development shoreline points were selected randomly across the entire southern coast of Louisiana that meet a minimum fetch distance of 4 km in at least one compass direction, including points that show no retreat during the given time interval. This fetch minimum was selected to eliminate small water bodies (e.g., marsh ponds and small lakes) where fetch and wave height is limited; based on sensitivity testing, 4 km is the point in the Young and Verhagen equation that wave power increases rapidly at a given water depth and at realistic wind speeds.

Gulf-fronting marsh shorelines such as the Chenier coast and the Bird's Foot Delta were excluded from this selection of shoreline points as wave power in these locations involves ocean swell as well as local, fetch-driven waves. The way in which these shorelines would be treated in this approach will be determined based on the results of the regression analysis (e.g., how variable retreat rates are among the other shoreline types and wave power conditions). Back barrier marsh retreat locations, which can be identified in the aerial photography, were not

included in the initial development of the regression rates as erosion rates may be influenced by barrier island processes other than wave power alone (e.g., overwash).

At each selected shoreline point, a remote sensing database was utilized to derive a fetch distance for each of 16 compass directions (every 22.5˚). An average water depth for each fetch was derived from the historical water depth information layer (Coastwide Reference Monitoring System (CRMS), 2008-2012) in the same database. Bathymetry included in the CRMS dataset consisted of data compiled from various sources, including single-beam sonar (NOAA, 1998), in situ soundings and model grids (Advanced Circulaion, ADCIRC SL16), and interpolations in areas with no existing data.

A shoreline orientation was selected to derive an angular relationship between shoreline compass direction and each wind compass direction for each model development point. This was necessary to correct for a reduction in wave power with increasing oblique wave direction relative to the shoreline (Marani et al., 2011; Trosclair, 2013). Wave refraction was not considered.

The final parameter necessary for the Young and Verhagen calculation is wind speed frequencies for each compass direction. Statistics for meteorological stations statewide (coastal and airport) that were active during the 2004-2012 period were compiled. GIS was used to assign the closest station to each of the 1,343 shoreline points used in this model development. Winds were corrected for anemometer height and sample averaging interval. Finally, wind data corresponding to time intervals for five major tropical events (e.g., Katrina and Rita in 2005, Gustav and Ike in 2008, and Isaac in 2012) were removed from the wind records, as they do not represent storm wave power at the model development shoreline point, and replaced using point-specific wave power calculated from the OWI storm wind fields utilized in ADCIRC hindcast models.

The final wave power, integrated over 2004-2012 for each marsh edge point, was calculated after correcting for wave orientation (for each compass direction) relative to the mean shoreline orientation. Mean shoreline orientation is computed via a GIS tool which calculates average orientation of a line segment. Individual wave power – marsh retreat rate regressions can be developed for individual marsh types/characteristics (e.g., 8 marsh types and 16 vegetation types, bulk densities, or organic matter content) using parameters in the United States Geological Survey National Wetlands Research Center database with appropriate groupings being determined by the regression analysis.

4.2.1 Fetch

Based on sensitivity tests, 4 km was selected as the minimum fetch over which waves of sufficient energy produce shoreline erosion. A GIS tool developed by the University of Washington was utilized to calculate fetch in 16 wind directions (UWWaves Toolbox for ArcGIS 9.0, 2005 David Finlayson). This tool calculates a Euclidean distance measured from each water pixel to land, but it can force the calculation of that distance to occur in specified wind directions. Figure 7 provides an example of the output of these calculations. This tool was run against a bathymetry-topography raster at 15 m resolution representing average conditions during the 2004-2012 time period. As the raster dataset contained more than 112 million pixels, fetch was calculated for each of those pixels, in 16 wind directions, for a total of approximately 1.8 billion calculations.

4.2.2 Shorelines Meeting the Minimum Fetch Criteria

The maximum fetch from the 16 wind directions was identified for each location. This maximum fetch raster was then overlaid on a land/water interface of coastal Louisiana to identify shorelines which are subject to a minimum of 4 km fetch. The shorelines that met the minimum fetch criterion are shown in Figure 8. Many smaller water bodies which occur throughout coastal Louisiana are not shown as they did not meet the fetch criterion. Figure 9 shows the selection erosion transacts.

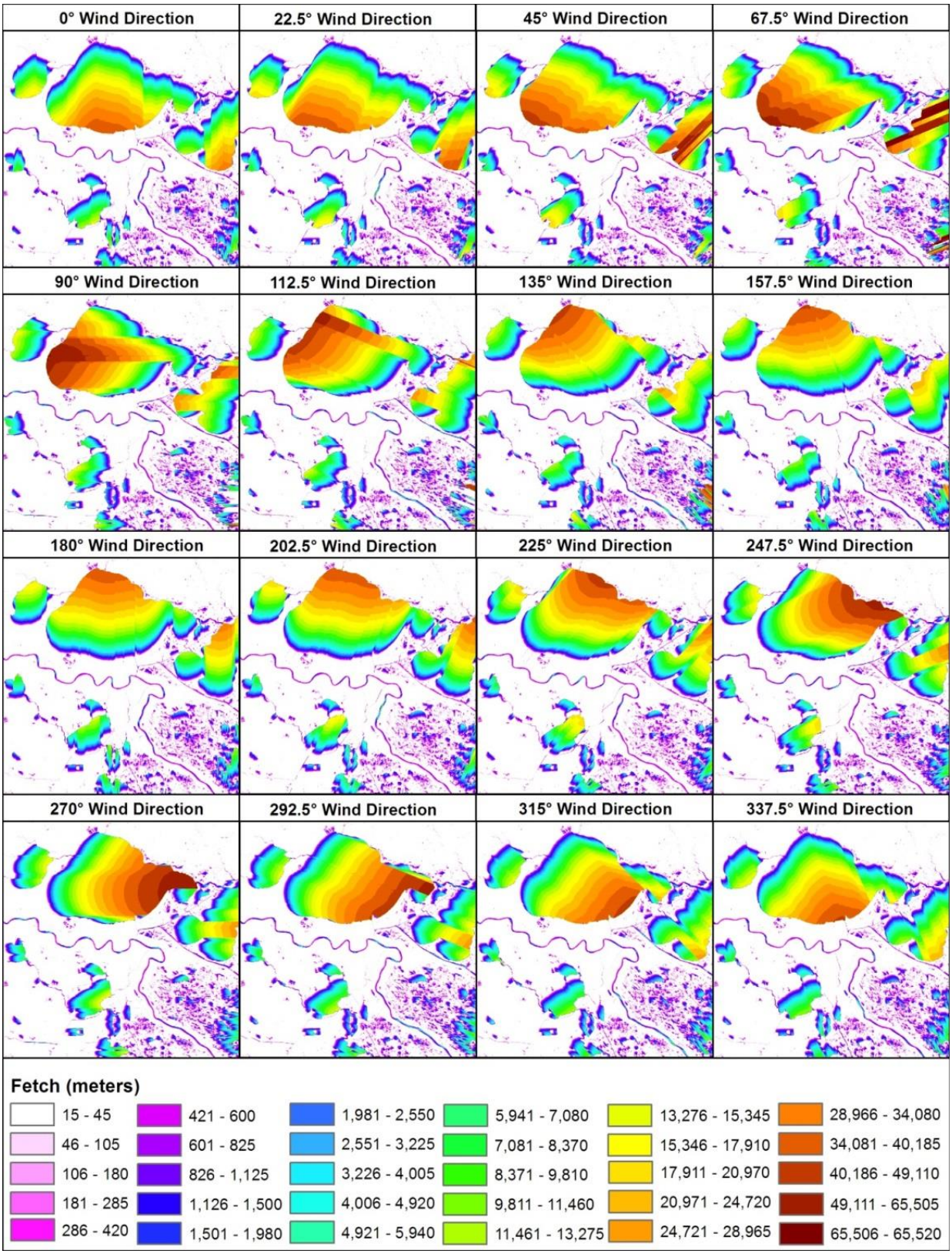

Figure 7: Calculated fetch for 16 wind directions for a portion of coastal Louisiana including Lake Pontchartrain and parts of the Breton and Barataria basins.

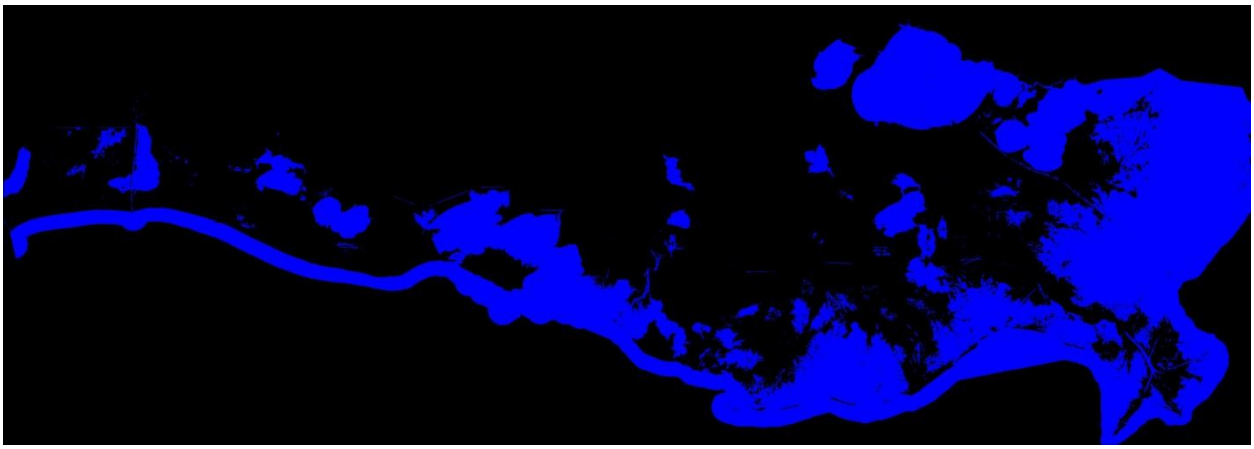

Figure 8: Coastal Louisiana shoreline which met the minimum 4 km fetch criterion. Shorelines (black) meeting the fetch criterion are bounded by blue open water bodies.

Figure 9: Shoreline erosion transect locations.

4.2.3 Random Site Selection

From the number of shoreline locations that meet the fetch criterion, a random stratified sample was taken. The sampling was stratified to ensure a representative distribution of points across areas of varying marsh type, bulk density, and erosion rates. One thousand points were initially selected using a random site selection tool, designed to include only points with a measurable retreat rate over the study period. Due to an initial concern of bias in the sample toward areas which had experienced shoreline erosion, 343 additional sites were selected at sites originally estimated to have undergone less shoreline erosion. Certain areas were deemed inappropriate for site selection including those influenced by a shoreline protection feature, a bulkhead, or other forms of armoring. Finally, ocean-fronting shorelines that experience ocean swell as well as local, fetch driven waves were excluded (e.g., Bird's Foot Delta, Chenier coast, Atchafalaya Bay; Figure 9). Back barrier marsh areas were also excluded as described in Section 4.0. As mentioned in that section, it is anticipated that the results of the regression can still be utilized in the ICM Barrier Island subroutine to produce a background erosion rate specific to this marsh type or bulk density that can be combined with the subroutine's calculation of overwash impact.

4.2.4 Transect Delineation

At these 1,343 sites, the location of the shoreline was manually delineated by placing a point or vertex at the initial shoreline and developing a transect from a line drawn perpendicular between the initial and final shoreline points. Points along the line were then included for each interim dataset. A resulting transect, as shown in Figure 10, would then contain three line segments that provide details of the distance between the shoreline position calculated for each of the intervals.

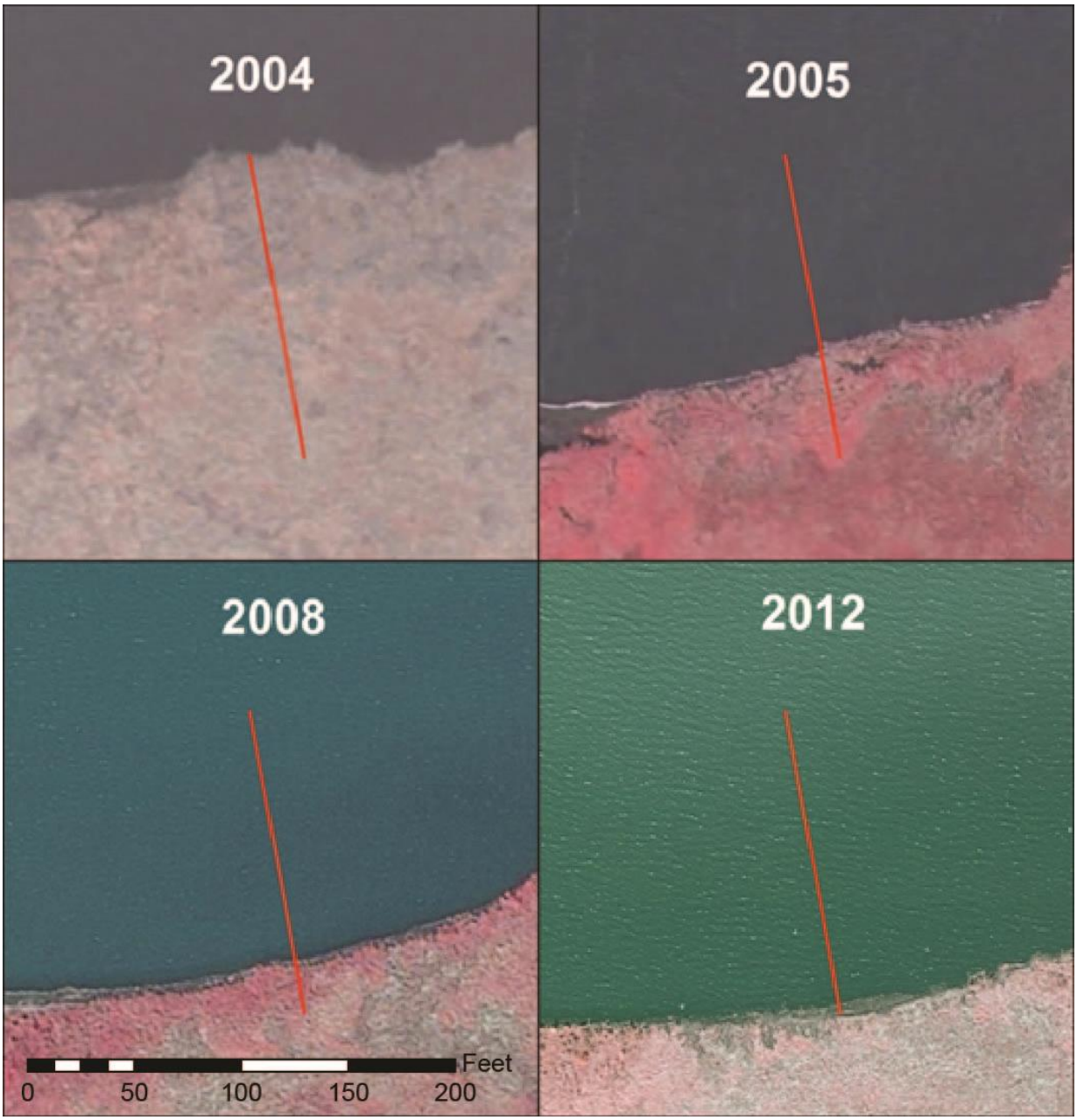

Figure 10: An example of a shoreline erosion transect and how the position changed in the 2004-2012 model development exercise interval. Note: 1 ft = 0.3048 m.

A tool to split line segments was then used so the length of each of these line segments could then be calculated in a Geographic Information System (GIS), namely ESRI ArcGIS, Split Line Segment. This calculation provided a distance of shoreline erosion during each time interval. That distance was used to estimate a shoreline erosion rate for each time period using exact decimal dates from the imagery date of acquisition (DOA). Site locations are shown in Figure 9.

The resulting database contained a rate of shoreline erosion for each time period, as well as an overall average between 2004 and 2012. These periods were selected to contain high and low hurricane activity as well as good quality imagery. Also provided were maximum fetch statistics for each of 16 wind directions at each site as shown in Table 4.

Table 4: Shoreline erosion transect database example.

Transect #	Erosion (m/y) 2004-2005	Erosion (m/y) 2005-2008	Erosion (m/y) 2008-2012	Mean Erosion (m/y) 2004-2012	Fetch (m) 0˚	Fetch (m) 22.5˚
1	11.9	2.8	3.9	5.1	18930	17310
2	6.3	2.4	6.4	5.0	18870	17970
3	6.4	2.3	2.4	3.2	18210	18480
4	4.4	4.0	3.4	3.8	18750	18210
5	17.4	6.9	6.0	8.6	18840	17100
6	13.3	5.3	3.7	6.2	18780	16980
7	14.8	5.6	7.9	8.5	18720	14760
8	6.4	2.6	1.8	3.0	15690	7590
9	6.1	2.0	1.7	2.7	15090	750
10	6.5	2.5	1.8	3.0	12600	3810
11	2.2	1.3	3.4	2.4	12030	2970
12	7.9	7.7	1.4	4.9	11460	1800
13	7.0	2.7	1.0	2.8	10650	900
14	3.2	7.9	2.3	4.4	6180	330
15	3.4	2.2	7.5	4.9	5730	300
16	1.7	4.4	0.7	2.2	3540	3180
17	3.2	0.7	2.5	2.0	2700	2820
18	1.3	0.5	0.7	0.7	2220	2340
19	1.9	0.8	1.7	1.4	1710	780
20	10.3	6.5	8.1	8.0	210	570

Also included in the database was location information, marsh zone (e.g., fresh, intermediate, brackish, and saline), marsh type (Table 4, as defined by Visser et al., 2013), and basin information.

4.2.5 Average Depth

A final data component necessary for the calculation of wave power was the average depth of water bodies (filtered tides) over the fetch in each of the 16 wind directions. Though bathymetry datasets are available, the calculation of depth across the 16 different fetches at each transect location is quite computationally expensive, and may prove difficult to incorporate into the final

2017 ICM. Therefore, two methodologies were employed for this exercise: a computationally intense method, and a simplified approach. Wave power – marsh retreat correlations were developed using both depth values to determine the sensitivity of the wave power to these depth calculation methods.

The simplified depth calculation was completed by determining the average water depth per open water compartment in the hydrologic model (the layout of the compartments shown in Figure 11). Each transect location (Figure 9) was linked to an open water compartment (Figure 11) and assigned the appropriate average water depth.

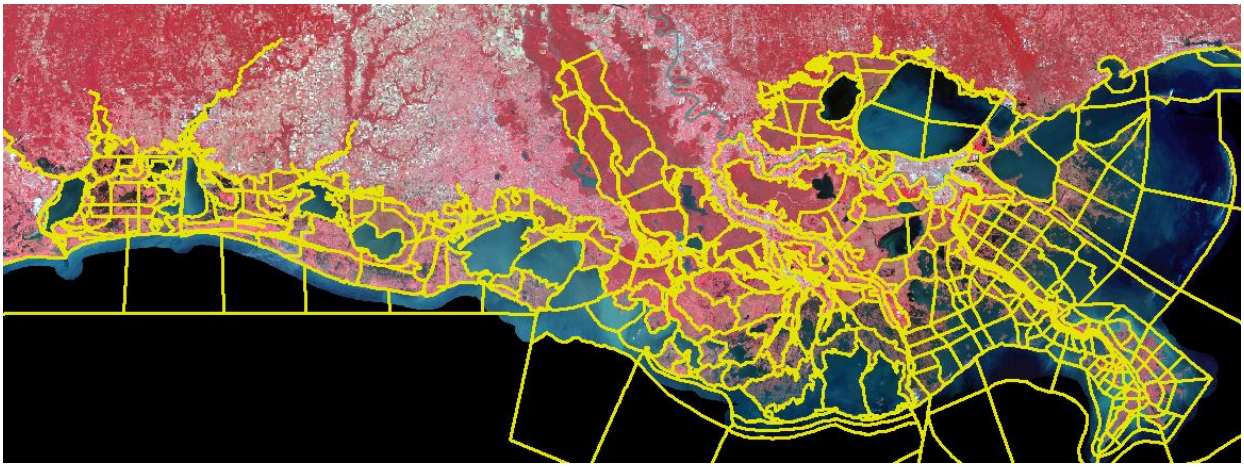

Figure 11: Hydrologic compartments for coastal Louisiana; current delineations used to determine average depth values.

The more rigorous but computationally complex approach included calculating the distance from marsh edge location to land in the 16 different wind directions, and using the bathymetry dataset to calculate average water depths across each of the 16 fetch directions at all 1,343 marsh edge locations.

An example of this approach is shown in Figure 12.

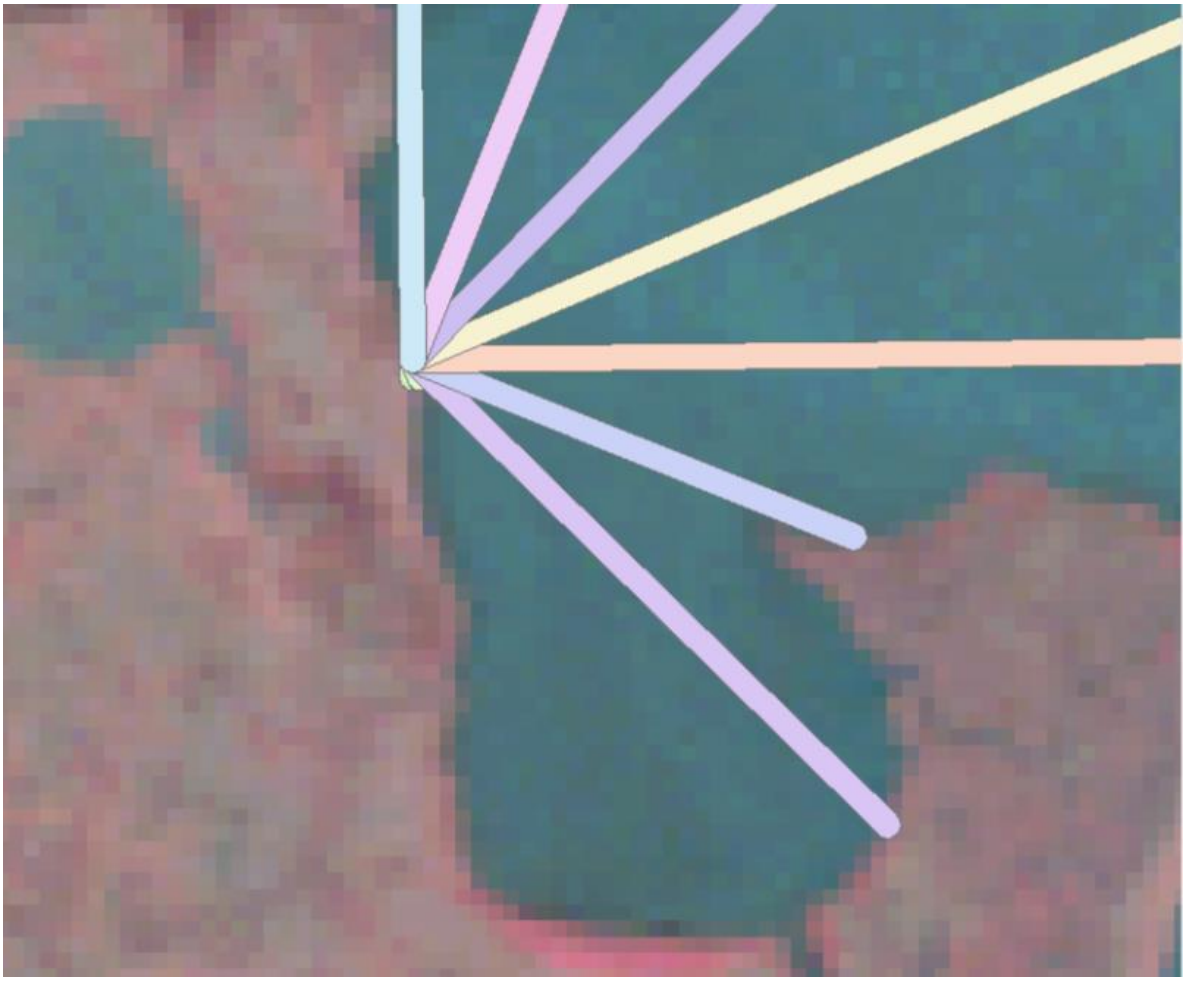

Figure 12: Approach used to calculate average water depth across the fetch in each wind direction.

In some wind directions, fetch was not calculated. This may have been because there was no water in a specific direction or a result of the alignment of the bathymetry data raster cells with regards to the wind direction alignment. Due to the inability of the geoprocessing routine to return a result in these cases, the average depth is unknown. Fetch directions where the results were unavailable were obtained from the simplified average water depth calculation described above.

In cases where either impounded water bodies with bottom elevations above the water level used in the analysis or some other geoprocessing artifact resulted in invalid depth estimates, the locations can be filled with an assumed small depth value of 0.5 m.

5.0 Code Development and Testing

5.1 Organization

As discussed in Section 3, the average wave power density was calculated in *R* using two separate methods: wind rose statistics were used for non-storm conditions, and wind timeseries

were used for the five hurricanes which occurred. Because there were separate methods for non-storm and hurricane condtions, two different functions were written in *R* to process the required input data for each method. Both of these functions utilize the same mathematical equations (provided in Section 3.2); however, due to the different formats used for the non-storm and hurricane wind datasets, different iterative schemes were required. A brief overview of the iterative schemes developed are provided in Sections 5.2 and 5.3.

The data sources that were described in previous sections (wind, retreat, fetch, depth, etc.) were organized into a variety of input data tables that were used by the *R* functions. Table 5 provides a brief description of these formatted data tables.

Table 5: Files used in *R* to calculate average wave power at each transect location.

Input files used for both non-storm and storm conditions	
Lookup_fetch.csv	Lookup table with fetch lengths in 16 compass directions for each transect
Lookup_depth.csv	Lookup table with average depth over the fetch in 16 compass directions for each transect
Lookup_transect_direction.csv	Lookup table with the marsh edge erosion direction for each transect
Input files used for non-storm conditions	
Lookup_wind_gage.csv	Lookup table with the wind station nearest to each transect
Station_files_intX.csv[1]	Table with the names for all files associated with each wind stations
YYYY_windrose_intX.csv[1,2]	Wind rose table for each wind station
YYYY_Median_intX.csv[1,2]	Table of median wind speeds for each wind rose
Input files used for storm conditions	
ZZZZ_wind_direction_degrees.csv[3]	Time series, at each transect, of the wind direction
ZZZZ_wind_speed.csv[3]	Time series, at each transect, of the wind speed
Output files	
Wave_Power_intX.csv[1]	Table of the average wave power for the entire non-storm period at each transect
Master_Table_intX.csv[1]	Table of variables and wave power values reported in wind rose direction/speed bins (not averaged together)
ZZZZ_ave_wavepower.csv[3]	Table of the average wave power over the hurricane
[1] X = interval number corresponding to remote imagery [2] YYYY = wind station name [3] ZZZZ = hurricane name	

5.2 Iterative Scheme Used for Wind Rose Tables (Non-Hurricane Conditions)

For each transect location:

1. Lookup direction of marsh retreat
2. Lookup wind gage name

3. Get wind rose table for respective wind gage
4. Get table of median wind speeds for respective wind rose

For each wind direction (dir) in the wind rose:

1. Lookup fetch distance
2. Lookup average depth over fetch

For each wind speed range (s) in wind rose:

1. Lookup portion of time observations were within direction/speed combination
2. Lookup median wind speed for direction/speed combination
3. Calculate equivalent fetch length, if needed (eqs. 15 - 18)
4. Calculate wave power for direction/speed combination (eqs. 3 – 14)
5. Weight wave power by portion of time observations were within direction/speed combination
6. Repeat steps 7 through 11 for each wind speed (*s*) in wind direction (*dir*)
7. Repeat steps 5 through 12 for each wind direction (*dir*) in wind rose
8. Sum weighted wave powers for each transect location
9. Repeat steps 1 through 14 for all transect locations

5.3 Iterative Scheme Used for Wind Time Series (One for Each Hurricane)

For each transect location:

1. Lookup direction of marsh retreat

For each time step:

1. Get wind speed from input data table
2. Get wind direction from input data table
3. Lookup fetch distance for respective wind direction
4. Lookup average depth over fetch for respective wind direction
5. Calculate equivalent fetch length, if needed (eqs. 15 - 18)
6. Calculate wave power
7. Repeat steps 2 through 7 for each time step
8. Take the mean of the calculated wave powers at the transect
9. Repeat steps 1 through 9 for all transect locations

5.4 Code Testing

Two steps were followed to ensure that the *R* functions were coded correctly and operating as designed. The first step was to have a team member who did not participate in the *R* coding review the code and ensure that the equations were entered correctly. This was done by a manual step-through of the *R* code, where each equation was compared to the mathematical equations as presented in this synthesis document (eqs. 2 through 18). If any discrepancies between the code and the synthesis document were found, the original literature source was referenced and corrections were made.

The second step of code testing and quality assessment was designed to ensure that the logic used to define the iterative schemes (see Section 5.3) was performing as originally planned. To accomplish this, intermediate tables were generated within the *R* function which saved the various calculated values to individual output files. The values generated via these intermediate calculations within the *R* function were then compared to the same terms manually calculated via an Excel spreadsheet. By comparing these values calculated via two separate methods, at a number of randomly selected transect locations, it was confirmed that the iterative scheme was working as planned.

6.0 Results

6.1 Wave Power: Marsh Retreat Rate Relationships

Linear regression analysis was used to compare relationships between wave power and marsh retreat rates using a number of different classifications schemes for the marsh shoreline characteristics including:

- Bulk density (BD) with sites separated into 0.1gm/cm^3 increments across the range of values
- Bulk density with sites grouped according to low (<0.4 g/cm^3), mid (0.4-0.6) and high (>0.6) categories
- Marsh type (Table 4)
- Vegetation type (Table 4)

Initial exploration of the data using all data points (see Figure 13 for an example) shows extensive scatter within the data set; Figure 13 also shows that including bulk density slightly improves the relationship but very high scatter still exists. Previous wave power - marsh retreat relationships (e.g., Marani et al., 2011; Trosclair, 2013) have shown a much narrower scatter of points (Figure 1). This may be because the Trosclair analysis is for a local site with short term direct measurements of waves that results in fewer extraneous factors influencing the data. Marani's study of Venice Lagoon (Italy), in contrast, used a much longer time period for the retreat rate calculations (1970-2004) so some variability which shows in our data may be masked, and in addition, Marani more accurately selected sites for the analysis deliberately excluded margins that are chiefly eroded by boat waves.

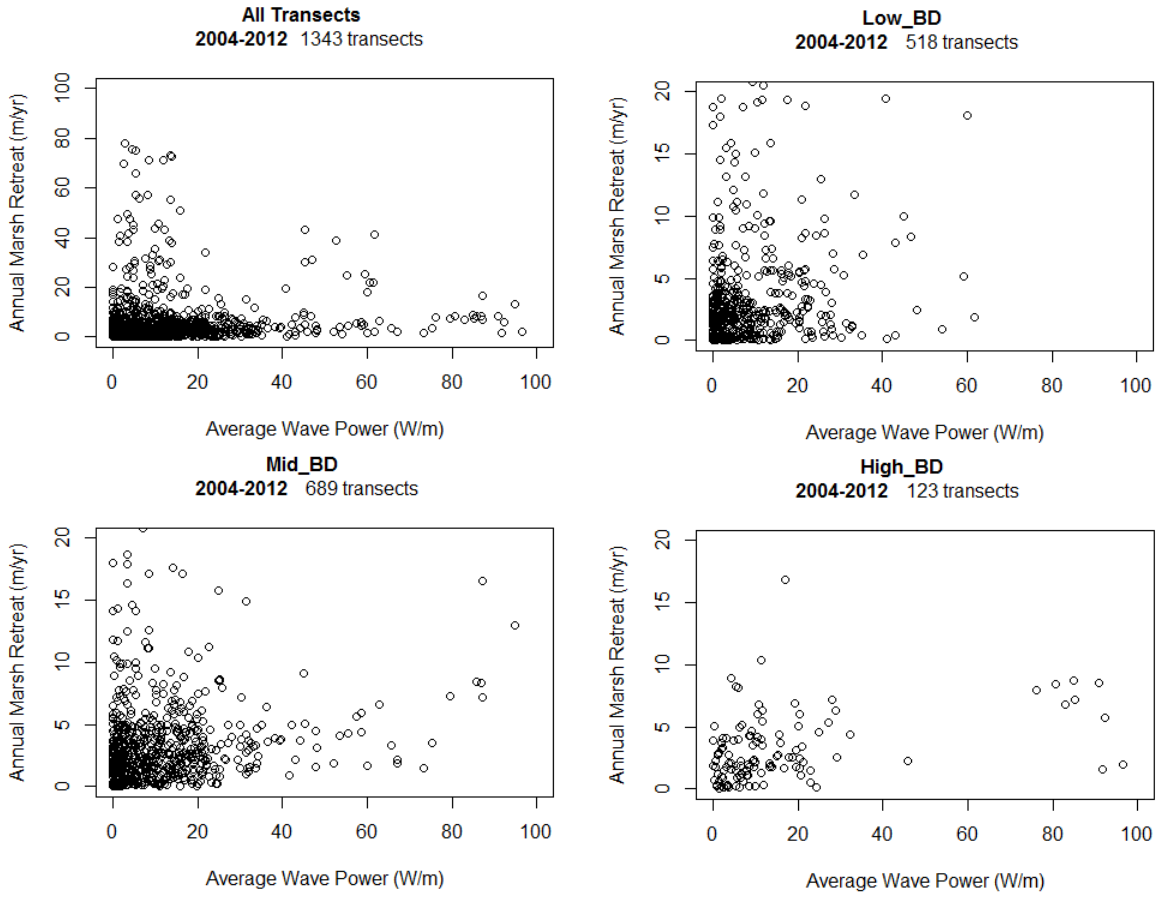

Figure 13: Plots of wave power density: marsh retreat rates. Top left graph is all 1,343 transects, other three graphs are separated by bulk density category (Low_BD, Mid_BD, and High_BD - see text for category intervals). Note that the y-axes for the bulk density subgroups are fixed and do not show the points above 20 meters of retreat per year.

Following a review of previous direct field assessments of marsh retreat rates, it was decided that using an upper threshold for marsh retreat would be a more reasonable approach than using all the data from the aerial photography analysis. In practice, ground-level measurements, as compared to those based on aerial imagery, are unlikely to be taken for marsh edges that appear to be uncharacteristic. Therefore, it is unlikely that the literature or data include uncharacteristically high retreat areas. Thus, an upper threshold for retreat rate data to be used in the regression analysis was identified based on a review of published values of marsh retreat in Louisiana. Following are four upper values of retreat from Louisiana studies.

- From Reed, 1989: 10 meters retreat over 21 months ~ 5.7 m/yr
- From Watzke, 2004: 13.3 meters retreat over 4.5 years ~ 3 m/yr
- From Trosclair, 2013: 1.5 meters retreat over 192 days ~ 2.85 m/yr (note these values are for marsh measurements, and the retreat rate of 6.5 m/yr noted earlier in this report also includes retreat of a mud scarp)
- From Melancon et al., 2013: TE-45 Terrebonne Bay Shoreline Protection Demonstration project preconstruction Reach A recorded the highest erosion rate from 1998-2005 of 5.7 m/yr

Thus, retreat rates greater than 10 m/yr were removed prior to conducting the regression analysis.

The results of the linear regression analyses for marsh type, vegetation type and the two approaches to bulk density are shown in Appendix 1. Averaging over bins of wave power density provided some improvement in the relationships but the scatter is still high (Figure 14). The use of the regression model within the ICM must be supported by the other subroutines to provide inputs as the landscape changes. While the ICM will provide an estimate of soil bulk density, the ability to resolve increments on 0.1g/cm^3 may be unreasonable in this type of large scale planning model. The R^2 values for the categories of bulk density are somewhat higher than for the vegetation and marsh classifications, but there is a lot of variability. In addition, the intercept values of approximately 2 m/yr are consistent with findings from field studies (Reed, 1989) that found erosion rates of up to 2/yr on relatively sheltered shorelines in Louisiana. This intercept accounts for the factors other than wind-driven wave power which may cause marsh retreat, such as boat wakes, sea level rise, biological activity, etc. Thus, the regression equations shown in Table 6 were the best that could be derived using this approach that are compatible with ICM application. These are based on the longest term measurements of retreat (i.e., 2004-2012) and generalized categories of bulk density that would be derived from other ICM subroutines.

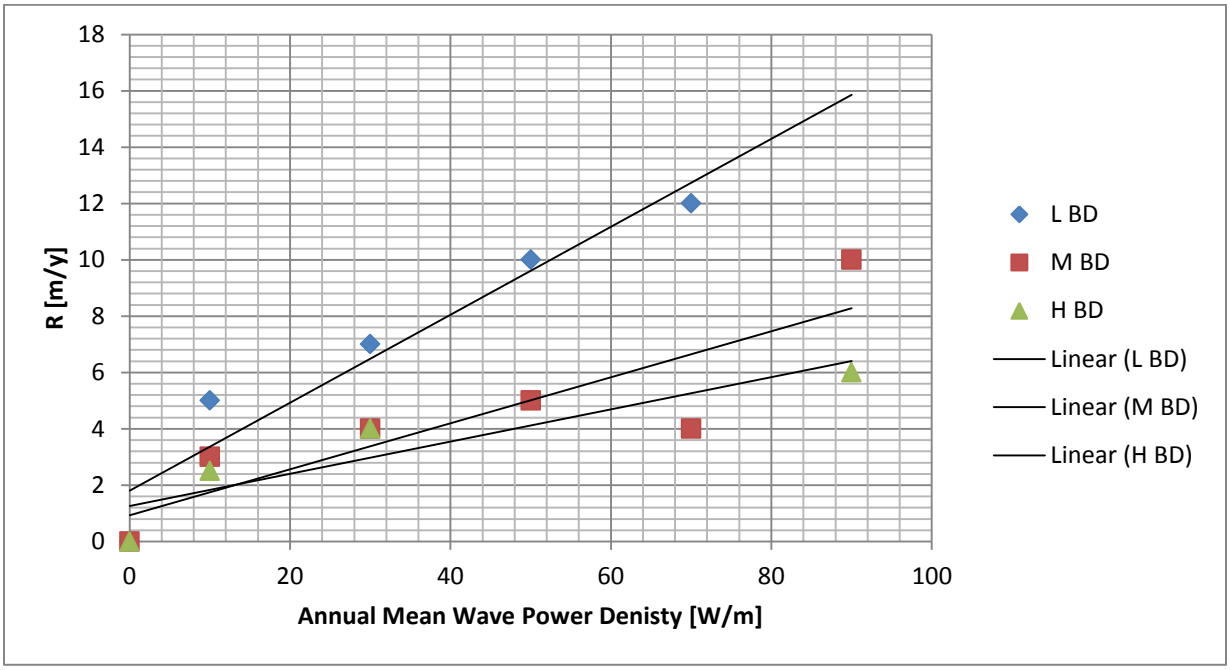

Figure 14: Regreassion of retreat rate aginst bulk density against binned wave power density. Low BD, Mid BD, and High BD - see text for category intervals.

Table 6: Possible Relationships to be used in ICM to calculate marsh retreat based on wave power.

Bulk Density Range	Intercept	Slope	R^2
Low (<0.4 g/cm^3)	2.03	0.05	0.04
Mid (0.4-0.6 g/cm^3)	2.49	0.03	0.04
High (>0.6 g/cm^3)	2.18	0.05	0.2

7.0 Alterative Approach: Raster Based Constant Edge Erosion Rate

7.1 General Approach

An alternative approach for estimating the average annual marsh edge erosion rate was developed because of the large scatter in the wave power density based regression equations in spite of the inclusion of factors such as marsh type, bulk density and vegetation type. In the alternative approach, the imagery data are used to determine current average annual marsh edge retreat rates.

Using an average marsh edge erosion rate per compartment results in all edges within the compartment eroding at the same rate, which would overestimate erosion in interior marsh ponded areas that are in the same compartments as larger open water bodies. Rather, raster data were developed that include spatially varied erosion rates, based on the data analysis described in Section 4, that do not vary over time. The erosion rate data was extrapolated to a 500-m resolution raster in order to ensure that the eroding shoreline stays within the raster extent throughout the 50-year model simulation, unless erosion rates are greater than 10m/yr which is considered rare (see Figure 15 and discussion in section 5.5 concerning measured marsh edge erosion rates).

The morphology subroutine in the ICM uses these marsh edge erosion rates to update the marsh edge location and the Digital Elevation Model (DEM), and the hydrology subroutine uses these observed rates to estimate the mineral mass available for deposition or transport throughout the hydraulic network. The annual retreat rate is used, in combination with organic matter and bulk density, to calculate an annual mass of inorganic sediment released and this is allocated to each time step equally. The released sediment is assumed to have the same grain size character as the sediment already in suspension. It is expected that as our knowledge of the wave interaction processes improves and as the database for the marsh characteristics improves, a more rational mechanistic model such as the wave power density approach can be implemented in the future.

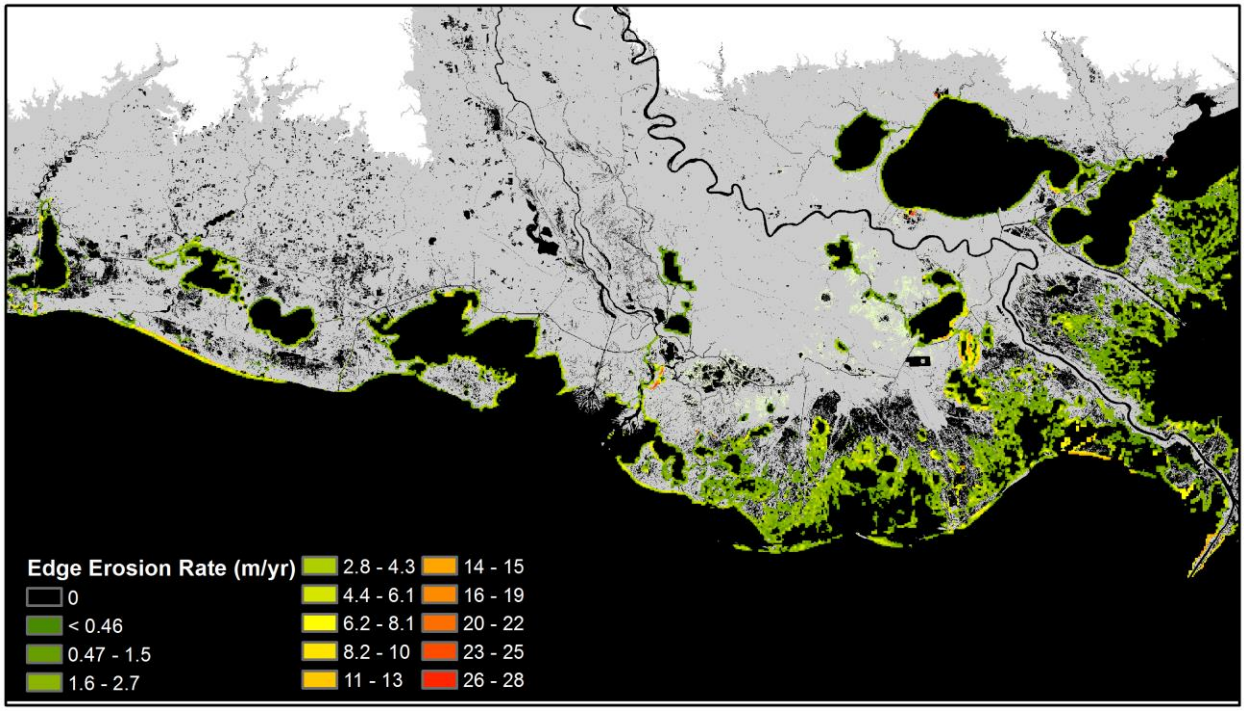

Figure 15: Example of raster data for spatially variable marsh edge erosion.

7.2 Treatment of Shore Protection and Bank Stabilization Projects

Marsh edge erosion can be reduced by the installation of on-shore or off-shore protection systems. In the 2017 Coastal Master Plan, these projects have been designated as: a) Shoreline Protection (SP), b) Bankline Stabilization (BS) and c) Oyster Reefs (OR). The general approach is to apply a 'wave erosion attenuation' attribute to the compartment or compartments containing the protection. A polyline is used to show the location of the protection. The influence of the protection will be designated by buffers which vary with the type of protection. The morphology subroutine will reduce the land loss within the buffer area consistent with the attribute value. This is reflected in the land-water ICM outputs as enough land is lost (or retianed) to adjust the land water map using the 30 m pixels.

The general procedure is as follows:

1) Generate buffers on landward side of SP, BS, and OR projects. Buffer distances are:

- 200 m for "off-shore" projects (shoreline protection and oyster reefs); the 200 m is based on buffers used for the 2012 Coastal Master Plan
- 0 m for "on-shore" projects (bank stabilization).

2) The raster data layer historic marsh edge retreat rate will be reduced for the impacted compartments. Each SP, BS, and OR project has an assigned 'wave' erosion attenuation attribute, which is used as the % by which to reduce the historic annual marsh edge erosion rate which is assigned using the raster.

8.0 Conclusions

Marsh edge erosion continues to be a substantial contributor to coastal land loss in Louisiana. At a local scale, it can be one of the most noticeable aspects of coastal land loss. The lack of explicit consideration of this factor in the analysis for the 2012 Coastal Master Plan was a concern, and this report has described the approaches which were considered as part of the Model Improvement Plan. Several others studies, cited in this report, have identified strong relationships between aspects of the wave regime and marsh shoreline erosion. The expectation was that it would be possible to develop such a relationship for coastal Louisiana. While estimates of wind/wave patterns across the coast can be developed, it appears that the diversity of shoreline conditions across the coast, including factors such as soil type, do not support the development of simple relationships. The insights gained from the analysis described in this report have been captured and could provide the basis for a more categorical approach to developing wave-erosion relationships in the future. However, if factors such as soil type are to be included then it will be important that others aspects of the modeling are able to predict changes in soil type at an appropriate resolution so that wave-erosion relationships can be actually applied in an integrated modeling framework.

The result of this work has been the application of spatially variable marsh edge erosion across the coast based on historical retreat rates. This not only allows the incorporation of this important process explicitly but enables improved evaluation of restoration projects that specifically target edge erosion. Future refinements may be needed as project evaluations are completed and the performance of this aspect of the modeling can be assessed.

9.0 References

Augustin, L.N., Irish, J.L., and Lynett, P. (2009). Laboratory and numerical studies of wave damping by emergent and near emergent wetland vegetation. *Coastal Engineering*, *56*, 332-340.

Cardone, V., and Cox, A.T. (2007). Tropical cyclone wind field forcing for surge models: Critical issues and sensitivities. *Nat. Hazards, 51,* 29–47.

Chen, Q. and Zhao, H. (2012). Theoretical models for wave energy dissipation caused by vegetation. *Journal of Engineering Mechanics—ASCE*, *138*, 221-229.

Cox, A. T., Greenwood, J.A., Cardone, V.J., and Swail, V.R. (1995). An interactive objective kinematic analysis system. *Proc. Fourth Int. Workshop on Wave Hindcasting and Forecasting*, Banff, AB, Canada Atmospheric Environment Service, 109–118.

Day, J.W., Shaffer, G.P., Britsch, L.D., Reed, D.J., Hawes, S.R., and Cahoon, D. (2000). Pattern and process of land loss in the Mississippi Delta: A spatial and temporal analysis of wetland habitat change. *Estuaries, 23*, 425-438.

Demirbilek, Z. and Vincent, C.L. (2002). Water Wave Mechanics. In *Coastal Engineering Manual, Part II, Water Wave Mechanics, Chapter II-1, Engineer Manual 1110-2-1100*, U.S. Army Corps of Engineers, Washington, DC.

Fagherazzi, S. and Wiberg, P.L. (2009**).** Importance of wind conditions, fetch, and water levels on wave-generated shear stresses in shallow intertidal basins, *J. Geophys. Res*., *114***,** F03022. doi:10.1029/2008JF001139.

Feagin, R.A., Lozada-Bernard, S.M., Ravens, T.M., Moeller, I., Yeager, K.M., and Baird, A.H. (2009**).** Does vegetation prevent wave erosion of salt marsh edges? *Proc. Natl. Acad. Sci. U.S.A., 106*, 10,109–10,113.

Filostrat, J. (2014). Internal Report on the Young and Verhagen Wave Model to Alex McCorquodale, Pontchartrain Institute for Environmental Sciences, University of New Orleans. Need copy of the reference

Francalanci, S., Bendoni, M., Rinaldi, M., and Solari, L. (2013). Ecomorphodynamic evolution of salt marshes: experimental observations of bank retreat processes. *Geomorphology, 195*, 53-65.

Gelina, P. and Quigley, R. (1973). The influence of geology on erosion rates along the north shore of Lake Erie. *Proceedings of the 16th Conference on Great Lakes Research*, 421-430, Int. Assoc. for Great Lakes Res., Ann Arbor, Mich.

Grabowski, R.C., Droppo, I.G., and Wharton, G. (2011). Erodibility of cohesive sediment: the importance of sediment properties. *Earth-Science Reviews, 105*(3–4), 101-120.

Holland, G. (1980). An analytic model of the wind and pressure profiles in hurricanes. *Mon. Wea. Rev*.108, 1212–1218.

Howes, N.C., FitzGerald, D.M., Hughes, Z.J., Georgiou, I.Y., Kulp, M.A., Miner, M.D., Smith, J.M., and Barras, J.A. (2010). Hurricane-induced failure of low salinity wetlands. *Proceedings of the National Academy of Sciences, 107*, 14014–14019.

Hsu, S. A., Meindl, E.A., and Gilhousen, D.B. (1994). Determining the power-law wind-profile exponent under near-neutral stability conditions at sea, *Applied Meteorology, 33*(6).

Jadhav, R.S., Chen, Q., and Smith, J.M. (2013). Spectral distribution of wave energy dissipation by salt marsh vegetation, *Coastal Engineering*., 77, 99-107.

Kamphuis, J. (1987). Recession rates of glacial till bluffs. *Journal of Water Port. Coastal Ocean Eng., 113,* 60-73.

Marani, M., D'Alpoas, A., Lanzoni, S. and Santalucia, M. (2011). Understanding and predicting wave erosion of marsh edges. *Geophysical Research Letters, 38*, L21401.

Mariotti, G. and Fagherazzi, S. (2010). A numerical model for the coupled long-term evolution of salt marshes and tidal flats*, J. Geophys. Res.*, *115*, F01004. doi:10.1029/2009JF001326.

Melancon, E. J. Jr., G. P. Curole, A. M. Ledet, and Q. C. Fontenot. 2013. 2013 Operations, Maintenance, and Monitoring Report for Terrebonne Bay Shore Protection Demonstration (TE-45), Coastal Protection and Restoration Authority of Louisiana, Thibodaux, Louisiana. 75 pp. and Appendices

Morton, R.A. and Barras, J.A. (2011). Hurricane impacts on coastal wetlands: a half-century record of storm-generated features from southern Louisiana. *Journal of Coastal Research, 27*, 27-43.

NOAA, (1998). *Estuarine bathymetric digital elevation models (30-meter resolution) derived from source hydrographic survey soundings collected by NOAA*. Silver Spring, MD: National Oceanic and Atmospheric Administration, National Ocean Service. Retrieved from http://estuarinebathymetry. noaa.gov; accessed on May 25, 2010.

Palaseanu-Lovejoy, M., Kranenburg, C., Barras, J.A., and Brock, J.C. (2013). Land loss due to recent hurricanes in coastal Louisiana. *Journal of Coastal Research, SI63*, 97-109.

Pant, H.R. (2013). *Erosional resistance of cohesive sediments in coastal saltmarshes* (Unpublished master's thesis). Department of Civil and Environmental Engineering, Louisiana State University, Baton Rouge, LA.

Penland, S., Wayne, L., Britsch, L., Williams, S., Beall, A., and Butterworth, V. (2000). Geomorphic classification of coastal land loss between 1932 and 1990 in the Mississippi river delta plain, southeastern Louisiana. *U.S. Geological Survey Open File Report,* 00–417.

Powell, M., Houston, S., and Reinhold, T. (1996). Hurricane Andrew's landfall in south Florida. Part I: Standardizing measurements for documentation of surface wind fields. *Wea. Forecasting*, *11*, 304–328.

Powell, M., and Houston, S. (1996). Hurricane Andrew's landfall in south Florida. Part II: Surface wind fields and potential realtime applications. *Wea. Forecasting*, *11*, 329–349.

Powell, M., Houston, S., Amat, L., and Morrisseau-Leroy, N. (1998). The HRD real-time hurricane wind analysis system. *J. Wind Eng. Indust. Aerodyn*, 77–78, 53–64.

R Core Team. (2013). *R: A language and environment for statistical computing*. R Foundation for Statistical Computing, Vienna, Austria. Retrieved from http://www.R-project.org/.

Resio, D.T., Bratos, S.M., and Thompson, E.F. (2002). Meteorology and wave climate. In *Coastal Engineering Manual, Meteorology and Wave Climate, Part II, Chapter II-2, Engineer Manual 1110-2-1100*, U.S. Army Corps of Engineers, Washington, DC.

Schwimmer, R. (2001). Rates and processes of marsh shoreline erosion in Rehoboth Bay, Delaware, U.S.A. *Journal of Coastal Research, 17*, 672-683.

Tonelli, M., Fagherazzi, S. and Petti, M. (2010). Modeling wave impact on salt marsh boundaries, *J. Geophys. Res., 115*, C09028. doi:10.1029/2009JC006026.

Trosclair, K.J. (2013). Wave transformation at a saltmarsh edge and resulting marsh edge erosion: observations and modeling. (Unpublished master's thesis). Department of Geological Sciences, University of New Orleans, New Orleans, LA.

Visser, J.M., Duke-Sylvester, S.M., Carter, J., and Broussard, W.P. (2013). A computer model to forecast wetland vegetation changes resulting from restoration and protection in coastal Louisiana. *Journal of Coastal Research, SI67*, 51-59.

Watzke, D.A. (2004). Short-term evolution of a marsh island system and the importance of cold front forcing, Terrebonne Bay, Louisiana. (Unpublished master's thesis). Department of Oceanography and Coastal Sciences, Louisiana State University, Baton Rouge, LA.

Wilson, C.A and Allison, M.A., (2008). An equilibrium model profile for retreating marsh shorelines in southeast Louisiana. *Estuarine, Coastal and Shelf Science, 80*, 483-494.

Young, I.R. and Verhagen, L.A. (1996). The growth of fetch limited waves in water of finite depth: Part 1. Total energy and peak frequency. *Coastal Engineering, 29*, 47-78.

Appendices

Appendix 1: Regressions by Bulk Density, Vegetation, and Marsh Type

Regressions Grouped by Bulk Density Value																
	2004-2012				2004-2005				2005-2008				2008-2012			
Bulk Density (g/cm^3)	#Transects	Intercept	Slope	R^2	#Transects	Intercept	Slope	R^2	#Transects	Intercept	Slope	R^2	#Transects	Intercept	Slope	R^2
0.2	86	1.92	0.05	0.02	86	1.91	0.05	0.02	86	1.92	0.05	0.02	86	1.94	0.05	0.02
0.3	195	2.29	0.01	0.00	195	2.27	0.02	0.01	195	2.46	0.00	0.00	195	2.29	0.01	0.00
0.4	238	2.03	0.06	0.08	238	2.01	0.06	0.09	238	2.05	0.06	0.08	238	2.04	0.06	0.08
0.5	233	2.68	0.02	0.01	233	2.67	0.02	0.01	232	2.72	0.02	0.01	233	2.67	0.02	0.01
0.6	174	2.27	0.04	0.09	174	2.24	0.04	0.09	174	2.31	0.03	0.09	173	2.28	0.04	0.09
0.7	115	2.44	0.04	0.17	115	2.40	0.05	0.16	115	2.46	0.04	0.17	115	2.44	0.05	0.17
0.8	41	2.34	0.03	0.14	41	2.30	0.03	0.15	41	2.34	0.03	0.15	41	2.36	0.03	0.14
0.9	4	-0.69	0.18	0.55	4	-0.38	0.17	0.46	4	-0.61	0.17	0.53	4	-0.85	0.20	0.61
1.1	4	-0.06	0.35	0.63	4	0.62	0.25	0.53	4	0.01	0.33	0.61	4	-0.57	0.45	0.72
1.3	3	-2.11	0.48	0.95	3	-2.61	0.59	0.94	3	-1.84	0.41	0.96	3	-2.19	0.50	0.95

Regressions Grouped by Bulk Density Range																
	2004-2012				2004-2005				2005-2008				2008-2012			
Bulk Density Range	#Transects	Intercept	Slope	R^2	#Transects	Intercept	Slope	R^2	#Transects	Intercept	Slope	R^2	#Transects	Intercept	Slope	R^2
Low_BD	406	2.03	0.05	0.04	406	2.00	0.05	0.05	406	2.31	0.02	0.01	406	2.05	0.05	0.04
Mid_BD	575	2.49	0.03	0.04	575	2.48	0.03	0.04	574	2.53	0.03	0.04	574	2.49	0.03	0.04
High_BD	116	2.18	0.05	0.20	116	2.13	0.05	0.20	116	2.19	0.04	0.20	116	2.20	0.05	0.20

Regressions Grouped by Vegetation Type																
	2004-2012				2004-2005				2005-2008				2008-2012			
Vegetation Type	#Transects	Intercept	Slope	R^2	#Transects	Intercept	Slope	R^2	#Transects	Intercept	Slope	R^2	#Transects	Intercept	Slope	R^2
Wiregrass	341	2.38	0.02	0.01	341	2.38	0.02	0.01	340	2.52	0.01	0.00	341	2.39	0.02	0.01
Bulltongue	35	1.43	0.02	0.01	35	1.39	0.03	0.01	35	1.46	0.02	0.00	35	1.43	0.02	0.01
Roseaucane	41	1.76	0.05	0.28	41	1.76	0.05	0.26	41	1.78	0.04	0.28	41	1.74	0.05	0.28
Cattail	3	0.69	0.00	0.00	3	0.58	0.03	0.01	3	0.70	0.00	0.00	3	0.69	0.00	0.00
Cutgrass	12	0.75	0.07	0.21	12	0.60	0.07	0.23	12	0.95	0.05	0.18	12	0.69	0.07	0.23
Delta Splay	9	2.22	0.21	0.08	9	2.07	0.20	0.08	9	2.17	0.21	0.09	9	2.38	0.20	0.08
Maidencane	18	1.77	0.01	0.02	18	1.76	0.01	0.02	18	1.78	0.01	0.01	18	1.77	0.01	0.02
Thin Mat	22	2.51	0.01	0.00	22	2.50	0.01	0.00	22	2.56	0.00	0.00	22	2.50	0.01	0.00
Needle Grass	11	0.10	0.22	0.33	11	0.30	0.24	0.50	11	0.13	0.21	0.33	11	0.40	0.19	0.24
Oystergrass	568	2.33	0.05	0.09	568	2.30	0.05	0.08	568	2.35	0.05	0.09	567	2.34	0.05	0.08
Saltgrass	6	0.82	0.04	0.41	6	0.83	0.04	0.39	6	0.85	0.03	0.40	6	0.82	0.04	0.41

Regressions Grouped by Marsh Type																
	2004-2012				2004-2005				2005-2008				2008-2012			
Marsh Type	#Transects	Intercept	Slope	R^2	#Transects	Intercept	Slope	R^2	#Transects	Intercept	Slope	R^2	#Transects	Intercept	Slope	R^2
Brackish	344	2.37	0.02	0.02	344	2.37	0.02	0.02	343	2.52	0.01	0.00	344	2.38	0.02	0.01
Intermediate	76	1.49	0.05	0.23	76	1.48	0.06	0.22	76	1.53	0.05	0.23	76	1.48	0.06	0.24
Forested	12	0.63	0.17	0.22	12	0.80	0.15	0.20	12	0.48	0.18	0.26	12	0.78	0.16	0.20
Fresh	64	2.19	0.02	0.02	64	2.15	0.02	0.02	64	2.23	0.02	0.01	64	2.18	0.02	0.02
Saline	579	2.32	0.05	0.09	579	2.29	0.05	0.09	579	2.34	0.05	0.09	578	2.34	0.05	0.09